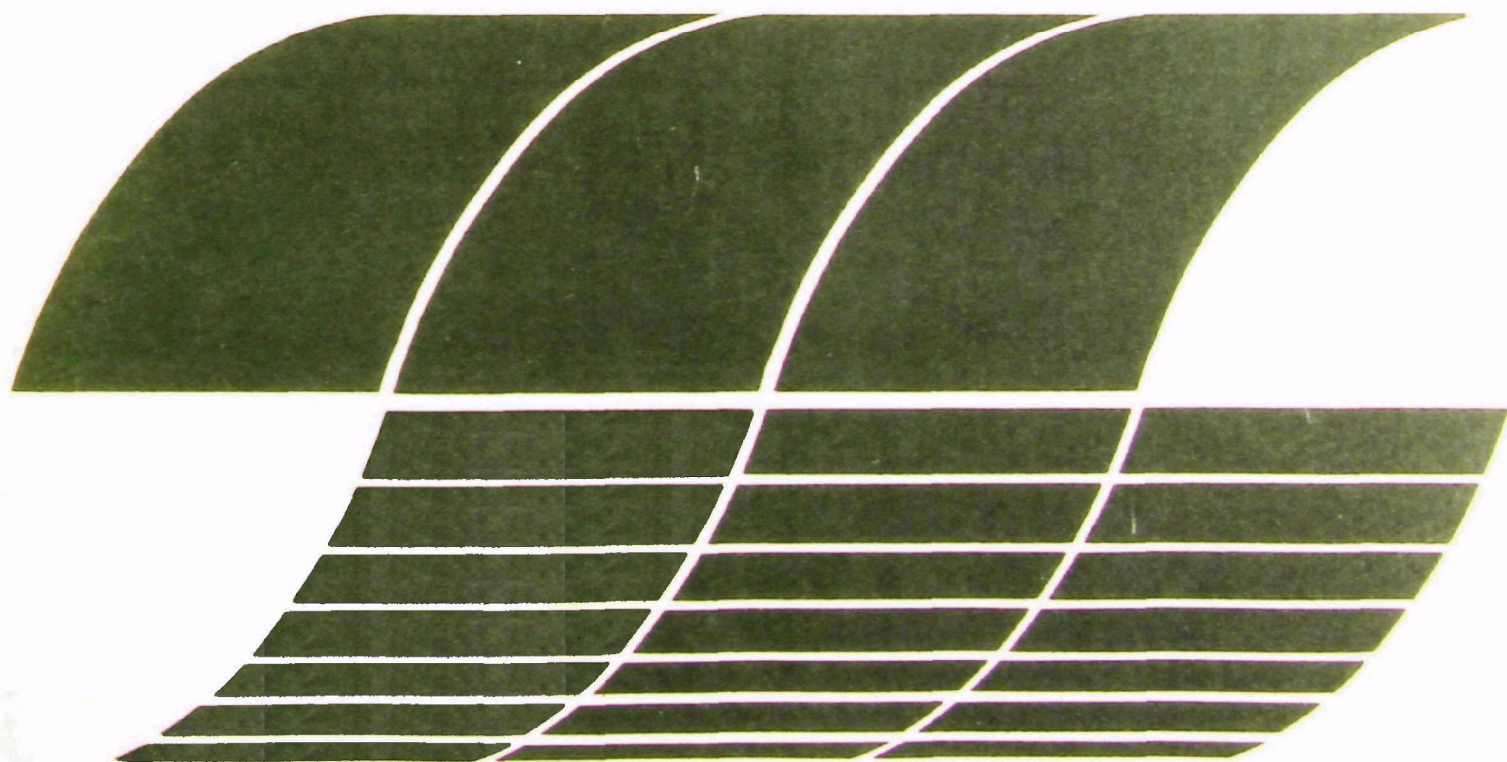




Effects of Interfacial Properties on Collection of Fine Particles by Wet Scrubbers

Interagency
Energy/Environment
R&D Program Report



RESEARCH REPORTING SERIES

Research reports of the Office of Research and Development, U.S. Environmental Protection Agency, have been grouped into nine series. These nine broad categories were established to facilitate further development and application of environmental technology. Elimination of traditional grouping was consciously planned to foster technology transfer and a maximum interface in related fields. The nine series are:

1. Environmental Health Effects Research
2. Environmental Protection Technology
3. Ecological Research
4. Environmental Monitoring
5. Socioeconomic Environmental Studies
6. Scientific and Technical Assessment Reports (STAR)
7. Interagency Energy-Environment Research and Development
8. "Special" Reports
9. Miscellaneous Reports

This report has been assigned to the ENVIRONMENTAL PROTECTION TECHNOLOGY series. This series describes research performed to develop and demonstrate instrumentation, equipment, and methodology to repair or prevent environmental degradation from point and non-point sources of pollution. This work provides the new or improved technology required for the control and treatment of pollution sources to meet environmental quality standards.

REVIEW NOTICE

This report has been reviewed by the U.S. Environmental Protection Agency, and approved for publication. Approval does not signify that the contents necessarily reflect the views and policy of the Agency, nor does mention of trade names or commercial products constitute endorsement or recommendation for use.

This document is available to the public through the National Technical Information Service, Springfield, Virginia 22161.

Effects of Interfacial Properties on Collection of Fine Particles by Wet Scrubbers

by

G.J. Woffinden, G.R. Markowski, and D.S. Ensor

**Meteorology Research, Inc.
P.O. Box 637
Altadena, California 91001**

**Contract No. 68-02-2109
Program Element No. EHE624A**

EPA Project Officer: D.L. Harmon

**Industrial Environmental Research Laboratory
Office of Energy, Minerals, and Industry
Research Triangle Park, NC 27711**

Prepared for

**U.S. ENVIRONMENTAL PROTECTION AGENCY
Office of Research and Development
Washington, DC 20460**

ABSTRACT

Typical wet scrubber models were analyzed to determine the effects of surface tension on particle removal efficiency. Particle capture (removal) is a two-step process: (1) collision of a particle with a spray droplet and (2) coalescence with the droplet. A change in surface tension of the scrubber water can influence both steps.

When the surface tension of scrubber water is reduced, spray droplets will normally decrease in size. The cumulative exposed droplet surface area is therefore increased. The larger exposed collection surface can improve collision efficiency. Too much reduction in droplet size, however, can actually reduce collision efficiency. One effect of surface tension in droplet-particle collisions is therefore to help optimize droplet size for maximum particle removal.

The coalescence process after a particle collides with a scrubber droplet has been described by the film thinning model. The model assumes that coalescence is controlled by the thinning rate of an air or vapor layer trapped between an impacting particle and droplet. If the film thins and ruptures before the particle rebounds, coalescence occurs. The thinning model predicts that a reduction in droplet surface tension allows deeper particle penetration into the droplet. The escaping vapor film therefore has a longer more resistive path, resulting in longer thinning times, thus reduced coalescence probability. The film thinning model is an instructive starting point but it needs to be modified if disagreement with experimental results is to be eliminated.

When the surface tension of a scrubber liquor is modified, collection efficiency may be slightly improved or degraded depending on the spray droplet sizes and the sizes of particles being removed.

CONTENTS

	<u>Page</u>
Abstract	iii
List of Figures	v
Acknowledgments	vii
List of Symbols	viii
<u>Sections</u>	
1. Conclusions	1
2. Recommendations	2
3. Introduction	4
4. Scrubber Models	5
5. Application of Surface Tension Results to Scrubber Models	9
6. Experimental Evaluations of Coalescence Theory	24
References	48
Appendix - Surface Tension Effects on Particle Collection Efficiency	51

FIGURES

<u>Number</u>		<u>Page</u>
1	Scrubber droplet size for maximum collection efficiency of particles 0.5 to 20 μm diameter, based on model ($V = 80 \text{ m/sec.}$)	10
2	Scrubber droplet size for maximum collection efficiency, based on model	11
3	Effect of surface tension on outlet particle concentration for 20 μm particles, typical of flyash	13
4	Effect of surface tension on outlet particle concentration for 0.8 μm diameter particles, typical of laboratory aerosol	14
5	Effect of surface tension on outlet particle concentration for 0.3 μm diameter particles, typical of cupola emission	15
6	Models for surface deformation	18
7	Coalescence efficiency vs velocity of impact of 134 μ droplets impinging on 2.2 mm drops: a) distilled water, $\sigma = 72 \text{ dyn cm}^{-1}$; b) 0.5% acetic acid solution, $\sigma = 70 \text{ dyn cm}^{-1}$; c) 5% acetic acid solution, $\sigma = 60 \text{ dyn cm}^{-1}$. Curve c) also resulted for distilled water when the drops were oppositely charged. (List and Whelpdale, 1969) ¹²	20
8	Inverted bubble	21
9	Film thinning model	22
10	High speed cine microscope equipment used for experimental evaluation of coalescence mechanisms	25
11	Glass rod with simulated flyash particle mounted on traversing mechanism	26
12	Traversing mechanism for impacting particles into water droplets	27
13	Coalescence of 1700 μm diameter glass particle with water droplet, 585 μsec delay, 6 cm/sec	30
14	Coalescence of 1000 μm diameter glass particle with water droplet, 780 μsec delay, 6 cm/sec	31
15	Coalescence of 725 μm diameter glass particle with water droplet, 468 μsec delay, 6 cm/sec	32
16	Coalescence of 275 μm diameter glass particle with water droplet, 351 μsec delay, 6 cm/sec	33

<u>Number</u>		<u>Page</u>
17	Coalescence of 100 μm diameter glass particle with water droplet, 156 μsec delay, 6 cm/sec	34
18	10 μm diameter glass fiber impacting distilled water droplet. Coalescence delay time ≤ 1 frame (i. e. , $< 39 \mu\text{sec}$).	35
19	Coalescence of 725 μm diameter glass particle with water droplet, 273 μsec delay, 42 cm/sec	36
20	Coalescence of 725 μm diameter glass particle with water droplet, 234 μsec delay, 42 cm/sec	37
21	Coalescence of 725 μm diameter glass particle with water droplet, 273 μsec delay, 42 cm/sec	38
22	Coalescence of 725 μm diameter glass particle with water droplet, 234 μsec delay, 42 cm/sec	39
23	Coalescence of 100 μm diameter glass particle with Freon TF, $< 39 \mu\text{sec}$ delay, 42 cm/sec	40
24	Coalescence of 100 μm diameter glass particle with water/surfactant, $< 39 \mu\text{sec}$ delay, 42 cm/sec	41
25	Coalescence of 100 μm diameter glass particle with water droplet, 156 μsec delay, 42 cm/sec	42
26	Comparison of theoretical predictions and experimental measurements of coalescence delay time for water at 6 cm/sec impact velocity	44
27	Comparison of theoretical predictions and experimental measurements of coalescence delay time for water at 43 cm/sec impact velocity	45
28	Comparison of theoretical predictions and experimental measurements of coalescence delay time for Freon-TF at 43 cm/sec impact velocity	46
29	Comparison of theoretical predictions and experimental measurements of coalescence delay time for water droplets containing surfactant and an impact velocity of 42 cm/sec	47

LIST OF SYMBOLS

A	--	Area of contact between a particle and a liquid droplet during collision
B	--	Correction factor in film thinning model
c	--	Constant
C_D	--	Cunningham correction factor
C_{DO}	--	Drag coefficient
d	--	Diameter of liquid droplets
D	--	Actual particle diameter
D_a	--	Aerodynamic diameter of a particle
f	--	Constant that may include effects of surface tension, particle growth, collection by means other than impaction, and other unknown parameters
F	--	Surface tension force
$F(K, f)$	--	Function of inertial parameter, k , and undefined factors, f
F_N	--	Resistive force exerted normal to the surface on a particle during collision with a liquid droplet
k	--	Inertial parameter
K_A	--	Constant
K_S	--	Harmonic oscillator constant. "Spring" constant in harmonic oscillator model of particle impact and bounce.
K_{PO}	--	Inertial parameter based on throat velocity
P	--	Average penetration of a particle into a water droplet during collision
Q_G	--	Volumetric flow rate of liquid phase
Q_L	--	Volumetric flow rate of gas phase
R	--	Particle radius
S	--	Constant depending on the shape of the depression in a water droplet made by an impacting particle

t	--	Thinning time of air or vapor film trapped between a colliding particle and a liquid droplet
v	--	Impact velocity
V_C	--	Critical impact velocity below which particle/droplet coalescence will not occur
V_G	--	Velocity of gas phase
V_{max}	--	Critical impact velocity above which particle/droplet coalescence will not occur
x	--	Radius of particle/droplet contact area
y	--	Penetration depth of particles into a liquid droplet during collision
β	--	A variable that includes all terms from Equation 5 that are functions of droplet diameter
γ	--	Constant depending on surface tension and particle size
δ	--	Thickness of vapor or air film at time of rupture
θ	--	Angle defining particle contact surface area
λ_0	--	Mean free path of molecules in the vapor film separating a particle and a water droplet
μ_G	--	Viscosity of gas
ρ_P	--	Particle specific gravity
ρ_L	--	Density of liquid
σ	--	Liquid surface tension
α	--	Liquid-gas flow rate parameter, $\frac{Q_L}{Q_G} \frac{\rho_L}{\rho_G}$

ACKNOWLEDGMENTS

The University of Washington, under an MRI subcontract, performed theoretical studies on the effects of surface tension on coalescence. This work was performed by Dr. John Berg and Scott Emory.

Gratitude is expressed to Patrick A. O'Donovan, Aerojet-General Corporation, for providing high speed photographic equipment used in these studies.

SECTION 1

CONCLUSIONS

1. Particle collection in a wet scrubber requires impaction and coalescence with a water droplet. A change in surface tension can affect both impaction and coalescence under some conditions.
2. Results of the theoretical study indicate that changes in surface tension of wet scrubber liquids can either improve or degrade particle impaction efficiency, depending on particle size and scrubber operating conditions; however, changes are expected to be small.
3. Current models describing coalescence do not agree well with experimental results so it is difficult to predict exact effects of surface tension on coalescence.
4. Theoretical results from this study can be used to imply relative effects of surface tension on scrubber performance, however additional experimental verification is needed.

SECTION 2

RECOMMENDATIONS

1. There is a large discrepancy between theoretical predictions based on the film thinning coalescence model and experimental results obtained. This discrepancy should be resolved by additional studies of the basic coalescence process. The discrepancy could be due to one of the following factors: assumptions in the film thinning model may be faulty, the film thinning mechanism may not be the controlling process, approximations used in the film thinning model may be too crude, or control of experimental conditions may have been inadequate.
2. Additional laboratory experiments will be required for theory modifications. These experiments should include:
 - Demonstration of the effects of particle materials other than silica, i. e., carbon and hydrocarbons.
 - Extension of coalescence measurements to smaller particles using higher optical magnifications and faster motion picture cameras. Present studies were limited to coalescence delay time measurements in the order of 150μ sec. Small particles as in a wet scrubber appear to coalesce in much shorter times. A 10μ m diameter particles, for example, might be expected to coalesce in 20μ sec, while a 1μ m particle might coalesce in approximately 4μ sec. Instrumentation with a 1μ sec resolution time, such as the Beckman and Whitley Model 189 framing camera, should be used.
 - Additional low surface tension liquids should be investigated in order to verify that the observed "surface tension effects" are real, and not due to some other property of the specific liquids that were used in this study. The other liquids should include (1) additional homogeneous compounds and (2) water with other surfactants.

- Water droplets have been observed to float for long periods on a water surface under controlled conditions. This phenomena cannot be adequately explained by the film thinning theory of coalescence. Additional studies, both theoretical and experimental, should be conducted to show the cause of these effects (e.g., surface tension, electronic polarizability, adsorbed monomolecular layers, or some other undefined mechanism) and whether they can be applied to scrubber models to improve collection efficiency. Results of such a study may also explain some of the differences observed between coalescence theory and experimental results.
3. Laboratory-scale scrubber experiments should be conducted to evaluate theoretical scrubber performance predictions based on models evolved under the present study. These experiments should show particle removal efficiency as a function of surface tension, droplet size, particle size, and relative impact velocity.

SECTION 3

INTRODUCTION

Wet scrubbers represent one of the primary methods for controlling particulate emissions from large industrial operations. Improvements in collection efficiency can reduce the size and capacity of the required control devices. Because of the high cost for a large control device, relatively small improvements can provide significant savings in original capital investment and in operating costs.

The objective of this study was to conduct a theoretical and experimental study to determine the effects of particle/liquid interfacial properties on the collection of fine particles by scrubbers and to apply results to analytical scrubber models.

The technical approach included the following steps:

- Analysis of current wet scrubber models
- Theoretical analysis of surface tension effects on particle collection efficiency
- Experimental testing of theoretical results
- Comparison of results with existing wet scrubber performance models

SECTION 4

SCRUBBER MODELS

The effect of surface tension is not explicit in most of the current wet scrubber analytical models. Penetration (one minus the collection efficiency) in the Calvert model for example, is given by Equation 1:

$$P = \exp - \left[\frac{2Q_L V_G \rho_L d}{55 Q_G \mu} \left| F(k, f) \right| \right] \quad (1)$$

where

P	=	average penetration
Q_G	=	volumetric flow rate of gas phase
Q_L	=	volumetric flow rate of liquid gas
V_G	=	velocity of gas phase
μ	=	viscosity of gas
ρ_L	=	density of liquid
d	=	diameter of liquid drops
F(k, f)	=	function of inertial parameter, k, and unknown factors, f

Surface tension, as such, is not one of the parameters listed; however surface tension influences droplet breakup and, therefore, the resultant droplet diameter, d. A reduction in droplet diameter improves collection efficiency by increasing the number of droplets and therefore the total exposed water surface area. The interfacial surface properties may also have a significant effect on the "F" factor because it is primarily a collection efficiency factor that included both collision and coalescence probabilities. It is assumed that surface tension does not have a direct effect on collision probability (other than that due to droplet diameter), but that it could have an effect on coalescence after impact.

Only limited experimental studies on the effects of surfactants in scrubbers have been performed. One is by Bughdadi.² He concluded that addition of surfactant (0.1 percent Triton CF-10) improved the collection efficiency of a venturi scrubber, especially at low liquid-to-gas flow ratios. He reported that the overall collection efficiency improved from 99.66 percent to 99.93

percent at 18ℓ water/28 m³ of gas (4 gal/1000 ft³). He attributed the improvement to easier penetration of the collected particulates into the scrubber water droplets, thus providing more effective wetting. He also observed a reduction in spray droplet sizes with surfactant additives. (It is difficult to explain the large change in penetration by collision processes alone.)

It has been shown experimentally that spray droplet size is proportional to the square root of the surface tension for sufficiently small liquid to gas ratios:

$$d = c \sigma^{1/2} \quad (2)$$

where d = droplet diameter
 c = constant
 σ = liquid surface tension

The maximum surface tension of scrubber water is approximately 72 dynes/cm (pure water). Additives and normal contaminants in operating scrubbers will typically reduce the surface tension to 50-60 dynes/cm. If a surfactant is added, the surface tension can be further reduced to 20-30 dynes/cm. Therefore, the maximum possible reduction, from 72 to 20 dynes/cm will reduce the spray droplet diameter by only 50 percent at most. In actual practice, a maximum reduction of 20 percent is more realistic. The effect of droplet size reduction on scrubber efficiency is not easily determined from the scrubber model, Equation 1. The droplet size affects the "F" factor which includes individual droplet collection efficiency and other unknown factors. Decreasing the size of droplets will increase the number of droplets so that droplet/particle collision efficiency will be improved, particularly for small particles. There is a practical limit, however, because when the droplets get small enough they may not be removed from the gas stream by the entrainment separator. The droplets in a scrubber are usually very large (on the order of 50 to 200μm diameter) compared to the particles being scrubbed (the most difficult particles to remove are typically 0.05 to 3.0μm diameter). When there is a large difference in size between the droplet and particle and the particle is in close proximity to the liquid surface, the droplet surface can be considered as an infinite flat plane.

4.1 Effect of Drop Size on Collection

Typically wet scrubber models have been described by Calvert, et al.¹ These models assume that impaction on the droplets is the only mechanism active in controlling the collection process. This is a good assumption if the particles are greater than 5 microns aerodynamic diameter and may be good for particles as small as one micron aerodynamic diameter.

Aerodynamic diameter is defined as:

$$D_a = \left(\rho_P C_D \right)^{1/2} D \quad (3)$$

where D = actual particle diameter
 C_D = Cunningham Correction Factor, a function of D , and the mean free path
 ρ_P = particle specific gravity

The scrubber models assume that the droplets are formed at a velocity much slower than the gas stream and the particles moving with the gas stream are collected as they impact the droplets. As the droplets are accelerated by the gas flow, the relative velocity decreases and they become progressively less efficient particle collectors. The collection efficiency typically approaches zero at the scrubber outlet. The models also assume that once a particle collides with a droplet, it invariably sticks. While intuitively reasonable, much evidence suggests that this assumption may need modification.

Surface tension enters into droplet size since the droplets are typically produced by atomization of the scrubber liquor introduced into the rapidly moving gas in the scrubber throat. The droplet size has been historically predicted by the Nukiyama and Tanasawa equation³, based on empirical work:

$$d = \frac{5.85}{V_G} \left(\frac{\sigma}{\rho_L} \right)^{1/2} + .0597 \left(\frac{\mu_L}{(\sigma \rho_L)^{1/2}} \right)^{.45} \left(\frac{1000 Q_L}{Q_G} \right)^{1.5} \quad (4)$$

d = drop diameter, cm
 σ = liquid surface tension, dyne/cm
 V_G = gas velocity, cm/sec
 ρ_L = density of liquid, g/cm³
 μ_L = viscosity of liquid, poise
 Q_L/Q_G = liquid to gas ratio, dimensionless

This correlation indicates that the droplet size is proportional to the square root of the surface tension for sufficiently small Q_L/Q_G . A number of other correlations have appeared in the literature showing a similar dependence.^{1,4}

Droplet size enters directly into scrubber performance models. Calvert's model¹ was selected as representative because it appears to be well constructed and to agree reasonably well with experimental data. For an infinite throat length and zero initial droplet velocity the model predicts a penetration as indicated in Equation 5:

$$P = \exp \left[- \alpha \frac{1}{C_{DO}} \frac{4K_{PO} + 4.2}{K_{PO} + .7} \frac{5.02 K_{PO}^{1/2} \left(1 + \frac{.7}{K_{PO}} \right) \tan^{-1} \left(\frac{K_{PO}}{.7} \right)^{1/2}}{1} \right] \quad (5)$$

where C_{DO} = drag coefficient
 K_{PO} = inertial parameter based on throat velocity
 $\alpha = \frac{Q_L}{Q_G} \frac{\rho_L}{\rho_G}$

The assumption of infinite throat length is good for small particles (less than 2 microns diameter) and/or small droplets (less than 50 microns diameter). In any case, the general dependence on droplet size is adequately indicated.

SECTION 5

APPLICATION OF SURFACE TENSION RESULTS TO SCRUBBER MODELS

The effect of changing droplet diameter on scrubber collection efficiency was calculated by combining all of the droplet size dependent terms in the scrubber model, Equation 5, into a single exponential factor, B.

$$B = 4 K_{PO} + 4.2 - 5.02 K_{PO}^{1/2} \left(1 + \frac{0.7}{K_{PO}} \right) \tan^{-1} \left(\frac{K_{PO}}{0.7} \right)^{1/2} \frac{1}{C_{DO}(K_{PO} + 0.7)} \quad (6)$$

Results indicate that for any given particle size to be removed, there is an optimum collection droplet size that will provide maximum collection efficiency. An example of the calculated results is shown graphically in Figure 1. The optimum droplet diameter is the point at which the collection efficiency exponent is the highest. Because the exponent is negative, a large absolute value represents a low penetration of particles.

The results given in Figure 1 assume an impact approach velocity of 80 m/sec. Calculations were also made for other velocities. The optimum droplet diameters for velocities ranging from 5 to 80 m/sec are plotted as functions of particle diameter in Figure 2.

It can be seen from the results in Figure 1 that a change in liquid droplet size may improve or degrade particle collection efficiency, depending on the initial sizes of the droplets and the particles being scrubbed. For example, 1μm diameter particles are removed most effectively by 40μm diameter droplets. If a scrubber produces 100μm diameter droplets, its collection efficiency for 1μm particles can be improved by reducing the droplet size to 40μm. If the scrubber initially produces 40μm diameter droplets either a reduction or an increase in droplet sizes will decrease the collection efficiency of 1μm diameter particles.

Generally, the penetration for large particles will be increased and that for small particles will be decreased when droplet sizes are reduced. The overall penetration will likely decrease since nearly all large particles will be collected in any case. If the scrubber is operating at near the optimum efficiency over most of the size distribution, changing the surface

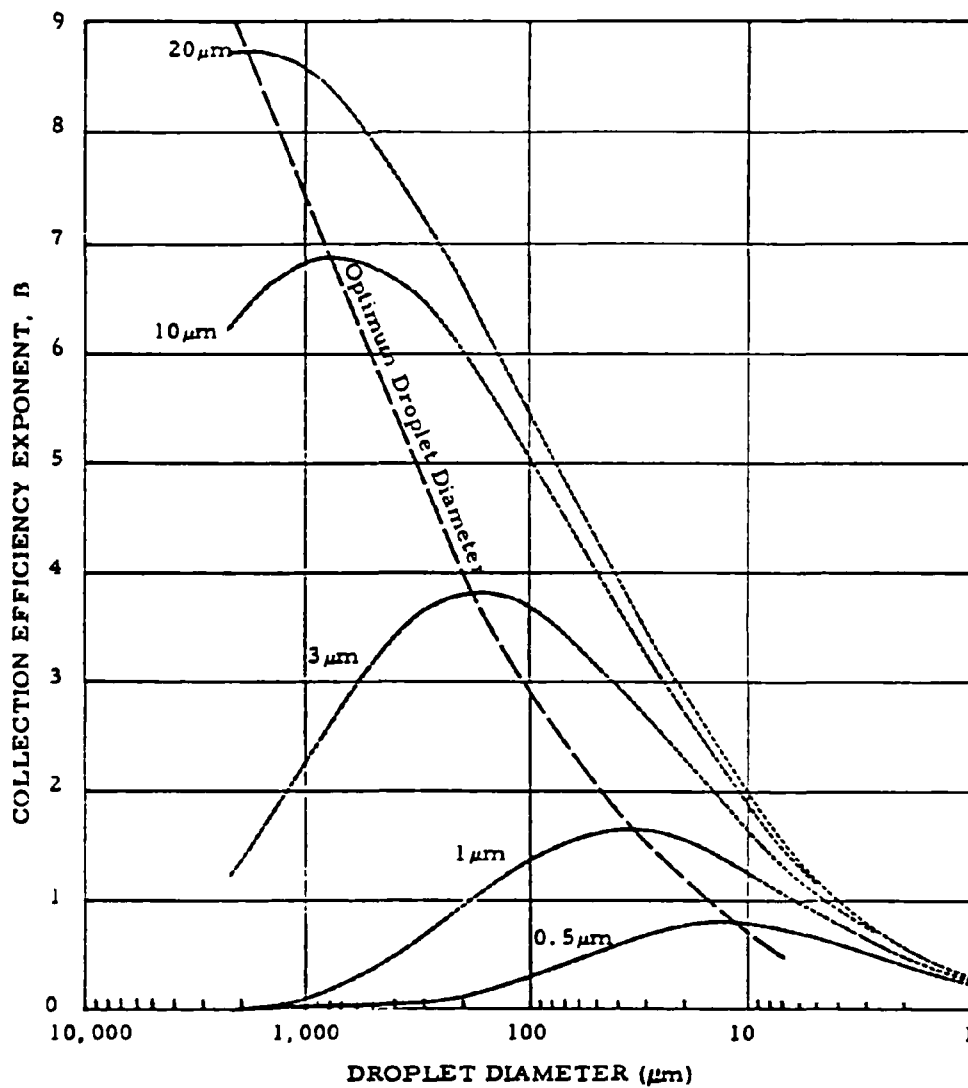


Figure 1. Scrubber droplet size for maximum collection efficiency of particles 0.5 to 20 μm diameter, based on model ($V = 80 \text{ m/sec.}$)

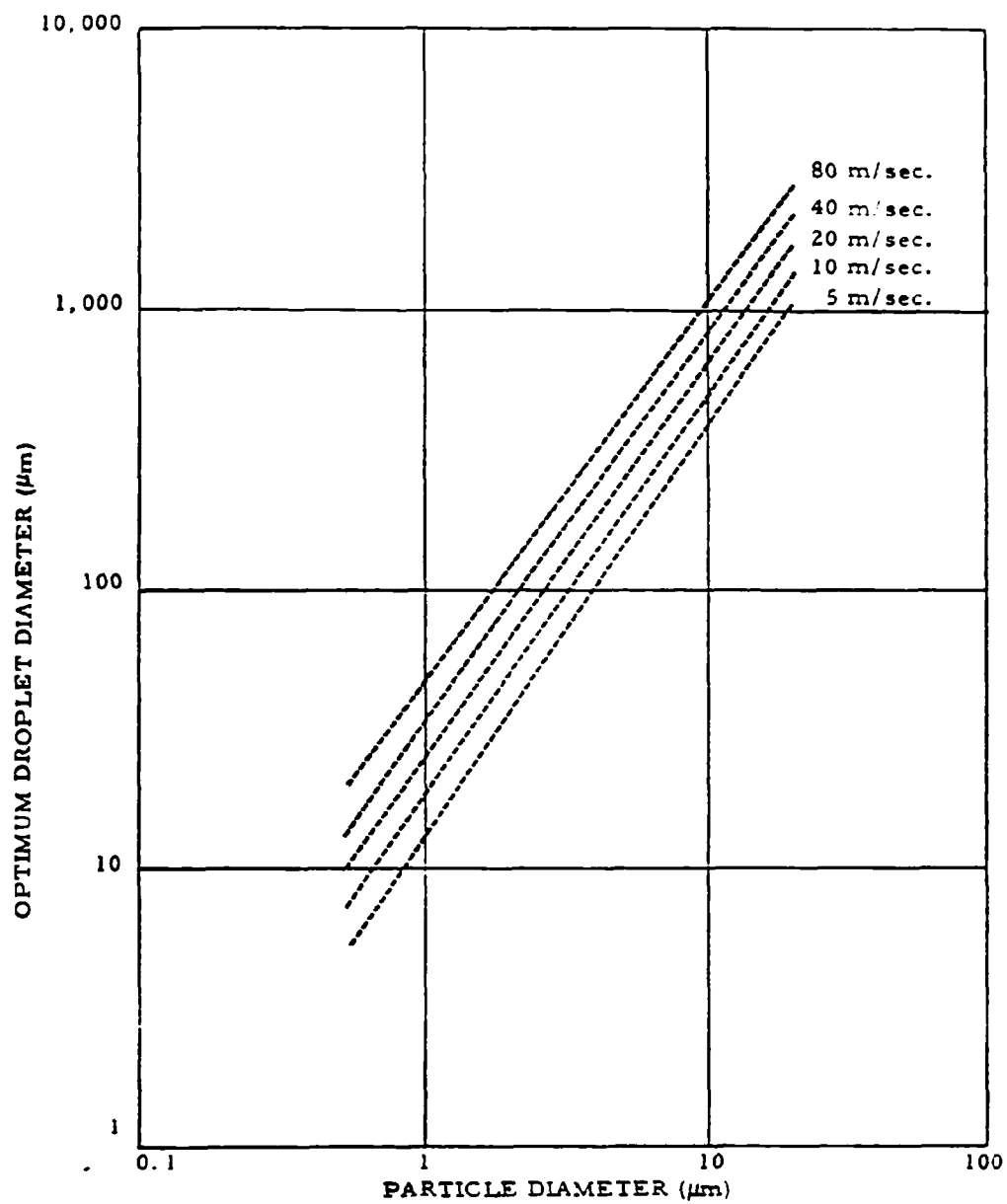


Figure 2. Scrubber droplet size for maximum collection efficiency, based on model.

tension is not likely to have much influence (if the coalescence properties remain unchanged) since the peaks in Figure 1 are fairly broad.

Table 1 shows the change in penetration for three different drop sizes assuming a reduction of the surface tension by a factor of 2, (the maximum likely due to addition of surfactant).

In this case the drop size was assumed proportional to the square root of surface tension and independent of the liquid to gas ratio. The initial drop sizes without surfactant are arbitrary. This table indicates the maximum change in penetration that could be expected due to surface tension variation. Actual changes in real scrubbers should be smaller.

TABLE 1. PREDICTED CHANGE IN SCRUBBER PENETRATION
DUE TO ADDITION OF SURFACTANT

throat velocity	=	8000 cm/sec
particle size	=	1 μ m (aerodynamic diameter)
penetration fraction without surfactant	=	.02

Drop Size Without Surfactant (μ m)	Drop Size With Surfactant (μ m)	B Without Surfactant	B With Surfactant	Fractional Penetration w/Surfactant
205	144	2.10	2.44	.011
144	102	2.44	2.70	.013
51	36	2.93	2.89	.021

Note that penetration is reduced by nearly a factor of 2 in the first two cases but increased slightly in the last. These calculations also indicate that if demisting is not a problem, a spraying device which produces smaller droplets than those indicated by Equation 4 could result in decreased penetration. Equation 4 predicts a drop size of about 125 microns.

Figures 3, 4, and 5 show changes in relative outlet concentration versus size and surface tension for typical scrubber parameters. The inlet size distributions are log normal with geometric mean diameters and standard deviations which correspond to typical flyash, lab aerosol, and cupola aerosol respectively. The distributions are normalized so that the peak value is 1000 and the area under the curves represents the total relative amount escaping the scrubber. The drop sizes were

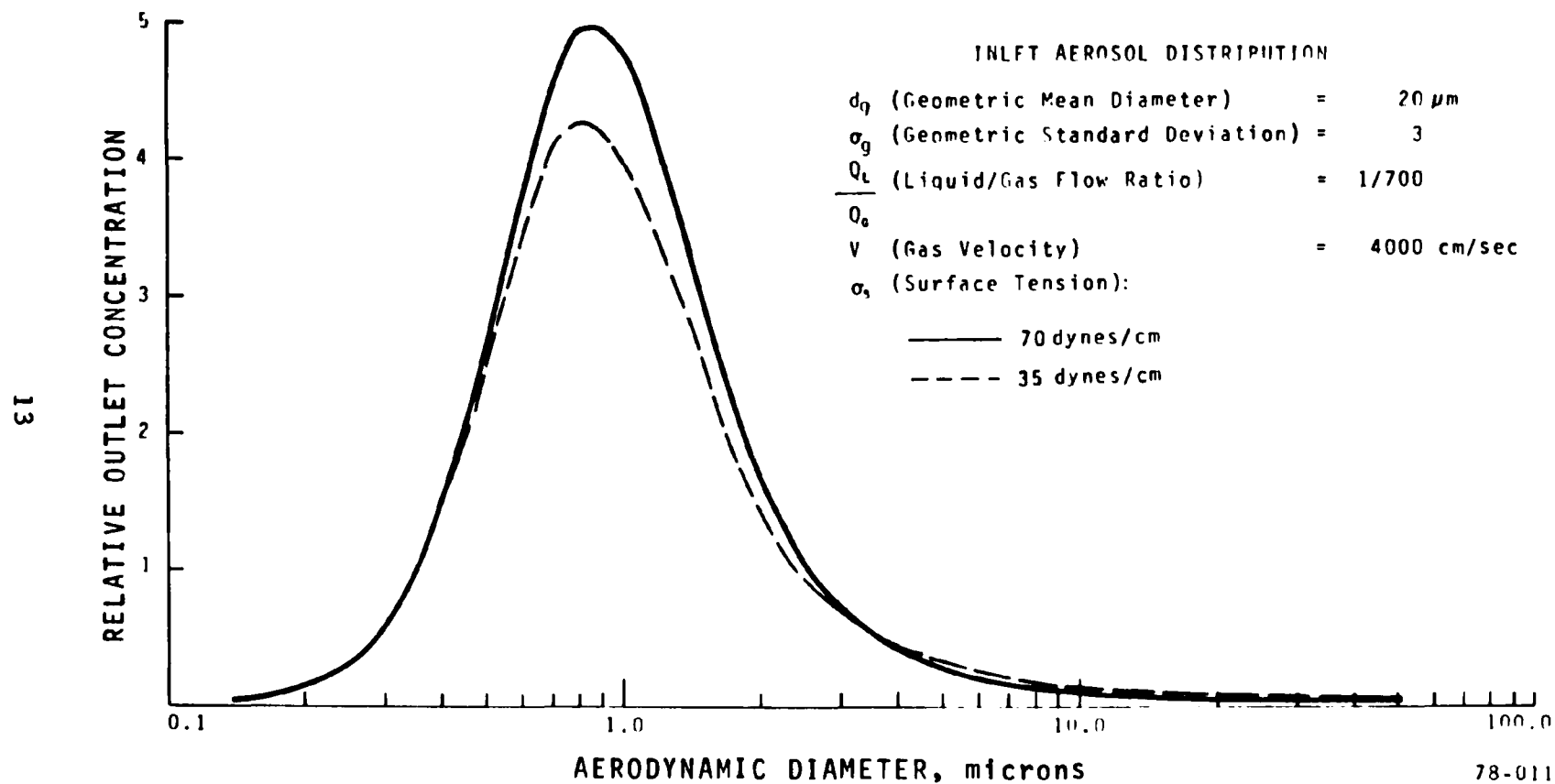
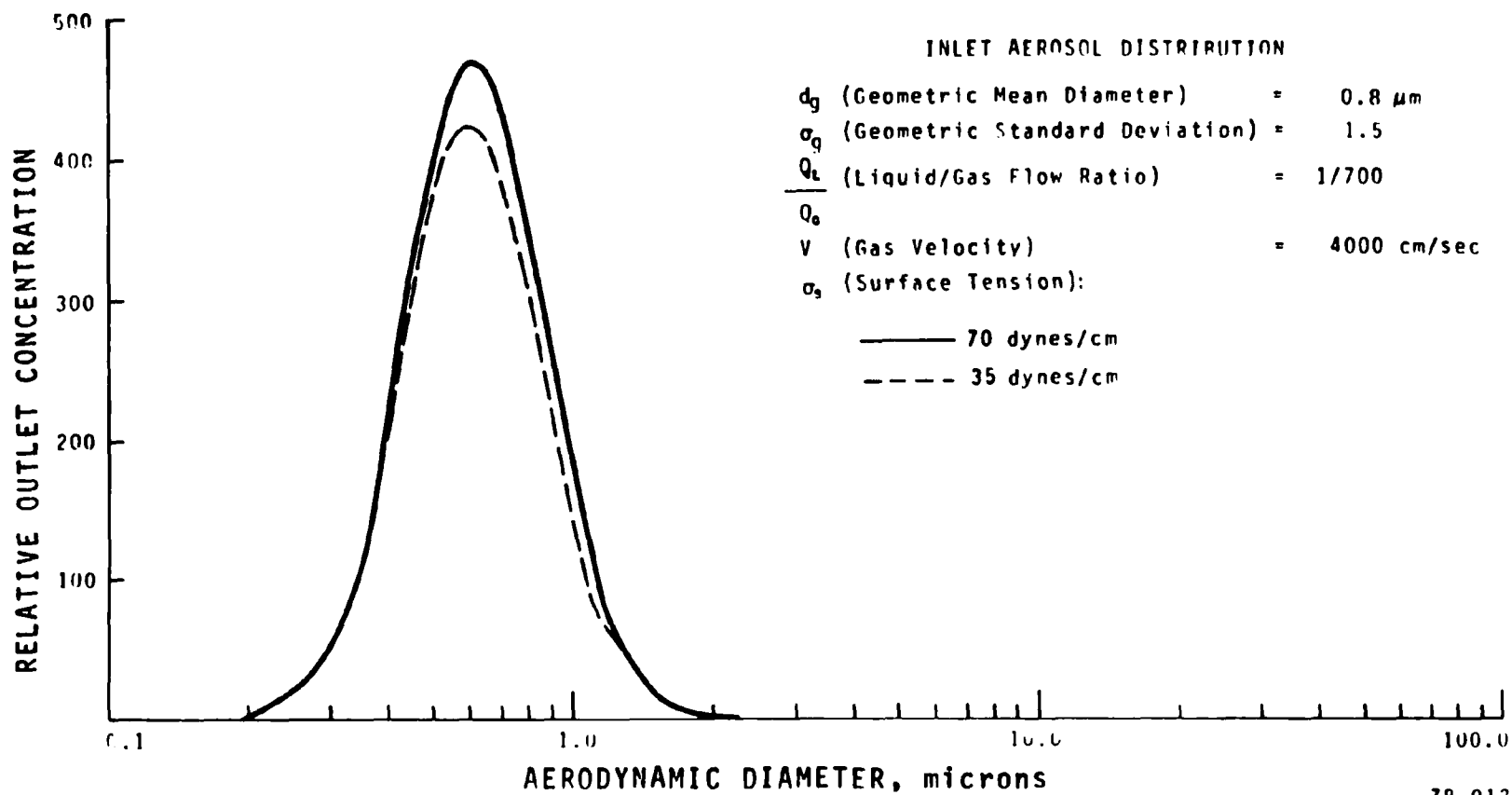


Figure 3. Effect of surface tension on outlet particle concentration for 20 μm particles, typical of flyash.



78-012

Figure 4. Effect of surface tension on outlet particle concentration for 0.8 μm diameter particles, typical of laboratory aerosol.

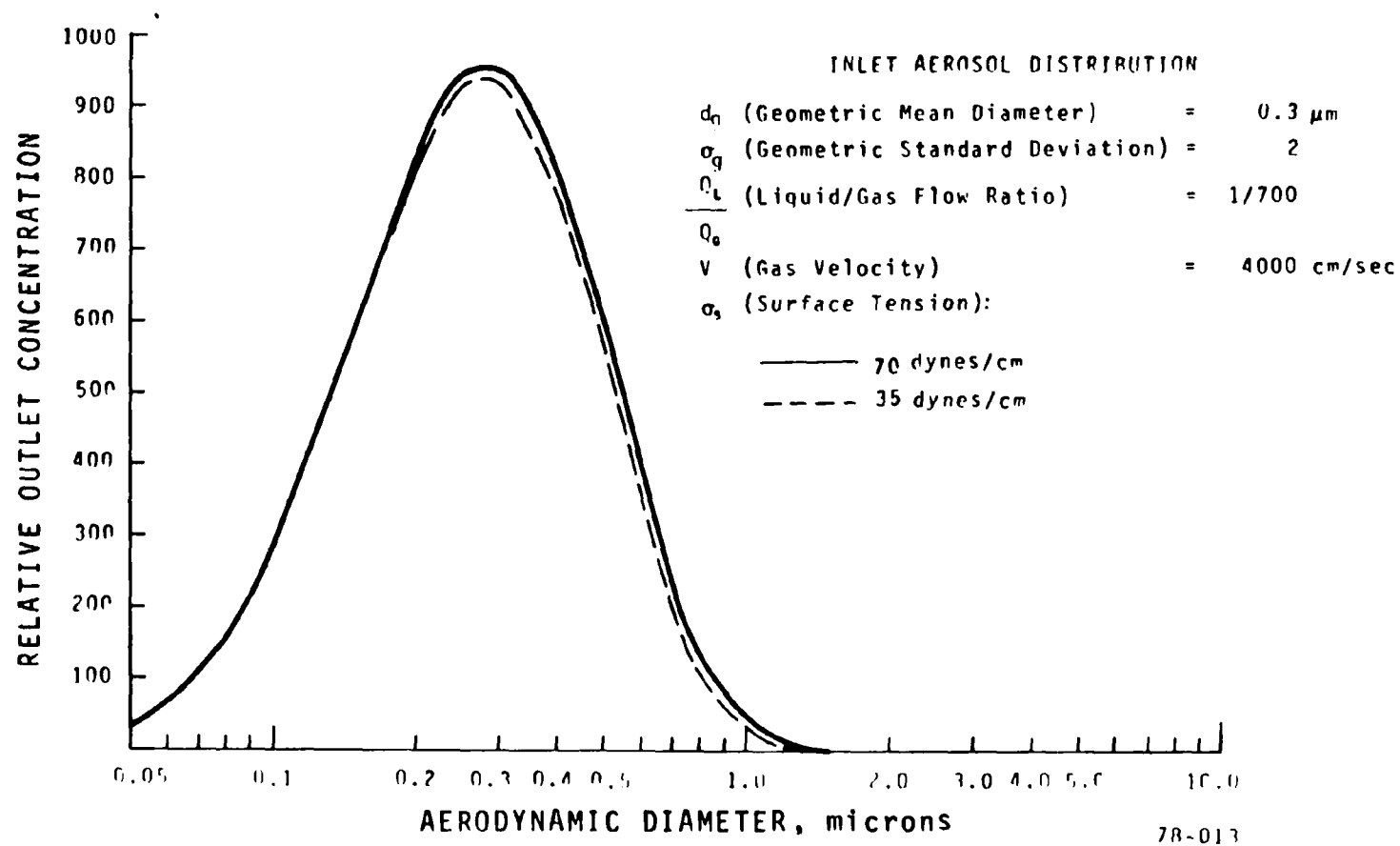


Figure 5. Effect of surface tension on outlet particle concentration for 0.3 μm diameter particles, typical of cupola emissions.

calculated using Equation 4 and are 173 and 143 microns for surface tensions of 70 and 35 dyne/cm, respectively. The drop size does not decrease by the square root of two as in Table 1 because of the presence of the surface tension in the denominator of the second term in Equation 4. The outlet concentrations decrease about 15 percent between 0.5 and 1.5 microns, a relatively small change in comparison to Table 1. The smaller change in penetration is due mainly to the smaller change in drop size. The results in Figures 3 to 5 are also typical of larger liquid to gas ratios and higher velocities. Note that the development of nozzles which produce smaller droplets have the potential of considerable improvement in scrubber performance.

Coalescence Effects

It has been observed that when two droplets or a particle and a droplet collide they sometimes bounce apart (Jayaratne⁵, Schotland⁶, Lobl⁷, Levin⁸). The most widely cited theory predicting whether coalescence will occur is the film thinning model.

The model assumes that as a particle collides with a water droplet, a thin layer of air or vapor is trapped between the particle and the deformed surface of the droplet. This air layer prevents immediate coalescence. The layer thins under the compression forces produced during the collision process; however, thinning is opposed by the layer's viscous forces. If the layer thins sufficiently before the colliding particle rebounds, the layer ruptures and coalescence occurs.

One serious problem is that the calculations based on this model, give results that are inconsistent with those observed by experiment. Secondly, due to the crude assumptions made in order to carry out the calculations, it is not currently possible to determine whether the inaccurate results are due to simplifying assumptions or because the thinning layer phenomenon is not actually the dominating process in coalescence.

The thinning layer model calculations are presented and discussed in detail in Appendix A. The salient feature of the way these calculations are performed is that the impact process is reduced to that of a simple harmonic oscillator with a "spring" constant given by Equation 7.

$$K_S = \frac{\sqrt{\frac{3\sigma}{R^3 \rho_P}}}{S} \quad (7)$$

where R = particle radius
 σ = droplet surface tension
 ρ_P = particle density
 S = a constant which depends only on the shape of
 the depression assumed to be made by the
 impacting particle.

For the model used by Lang⁹ and Emory¹⁰ S = 1. Jayaratne's more rounded depression is more realistic and gives an S = (1.6). The two shapes are shown in Figure 6.

Viscous forces acting in the liquid may also be considered. Emory¹⁰ indicates that they are several orders of magnitude less than the calculated surface tension forces, however, and they may be neglected for practical purposes. Emory¹⁰ and Arbel¹¹ also indicate that electric double layer forces are smaller than the surface tension forces and can be neglected.

Coalescence is assumed to occur if the layer thins to a rupture thickness δ before rebounding. δ is assumed constant. A condition for coalescence may be derived and the result is shown in Equation 8.

$$R^2 BV \leq \frac{8}{3} S \left(\frac{\sigma}{\mu_G} \right) \delta^2 \quad (8)$$

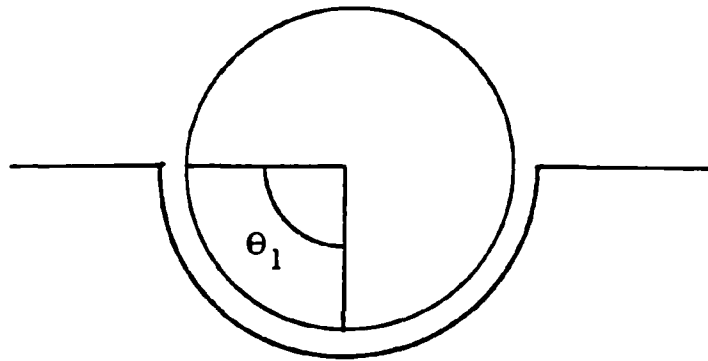
R = particle radius
 μ_G = gas viscosity
 B = an approximate correction factor used if δ is less than the
 mean free path, λ_0 ; $B \cong 0.71 (\delta/\lambda_0) [2 - 0.71 (\delta/\lambda_0)]$
 V = Impact velocity normal to the surface
 S = constant depending on the shape of the depression
 in a water droplet made by an impacting particle

Note that Equation 8 predicts that given a sufficiently small velocity, coalescence will always occur. However, above a certain velocity, V_{\max} , depending upon R, the particle radius, coalescence will not occur.

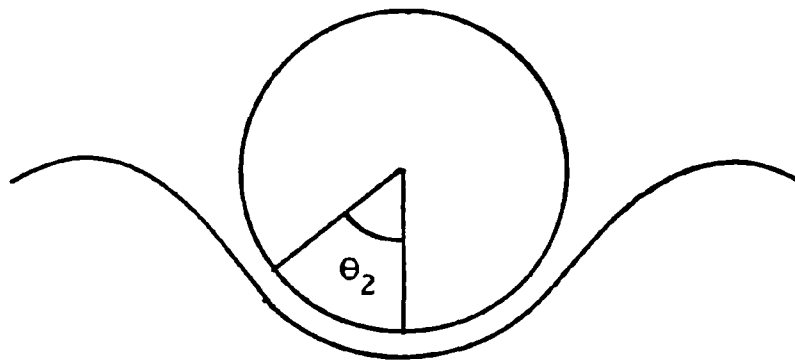
V_{\max} is obtained by dividing Equation 8 by $R^2 B$:

$$V_{\max} = \frac{8}{3} S \frac{\sigma}{\mu_G R^2 B} \delta^2 \quad (9)$$

The rupture thickness may be estimated from theoretical or experimental determinations. The fact that coalescence is impeded by increasing impact velocity seems intuitively incorrect and experiments confirm this



Model 1
Lang⁹, Emory¹⁰



Model 2
Jayaratne⁶

Figure 6. Models for surface deformation

intuition: Below a certain velocity, V_c , coalescence does not occur and above V_c it does (Schotland⁶, Jayaratne⁵, List²). In addition, the time for a colliding drop to rebound is strongly dependent on impact velocity as shown by Jayaratne⁵. The film thinning model described above predicts a rebound time independent of velocity (since the period of a simple harmonic oscillator is independent of its initial velocity). Lastly, the rupture thickness δ is in fact an arbitrary factor. Emory¹⁰ suggests 50 Å while Jayaratne suggests 1000 Å. This difference makes a factor of 400 difference in Equations 8 and 9.

The idea that a particle traps an air layer which impedes coalescence seems accurate intuitively, so the question remaining is what is wrong with current thinning layer models. The answer to this question is currently unresolved; however, the problems fall into three areas (or possibly a combination of the three).

1. Film thinning may not be the dominant process. Significant evidence exists to suggest this possibility. The most compelling results were obtained by List². Figure 7 shows coalescence efficiency for small droplets impacting upon a water surface. The addition of small and moderate amounts of acetic acid increases the coalescence at low velocities. These results suggest that surface forces are dominant and that, at least for low velocities, film thinning may not be a controlling factor. The thinning layer model depends only upon liquid density and square root of the surface tension of the liquid and these factors vary only a relatively small amount in Figure 7. Note that for a 5 percent acetic solution, coalescence occurred at all impact velocities.

If smaller water droplets fall onto a clean water surface from low heights, they float along the surface for a considerable length of time¹³, much longer than appears accountable by the film thinning model. Small amounts of detergent can greatly increase the life of these floating globules. Again, surface forces appear responsible. It is impossible to achieve the same effect with mercury drops on a clean mercury surface; however, a small amount of oil (dioctyl phthalate in this case) will stabilize small surface drops of mercury indefinitely (personal observation). Lastly, it is possible to create an "inverted bubble" in water¹⁴. If water is carefully dropped into a dish of soapy water, a drop may submerge itself surrounded by a thin layer of air. These "inverted" bubbles are stable until they drift upward and break against the surface. If a slightly more dense liquid drop is used it may sink and thus last for a considerable length of time.

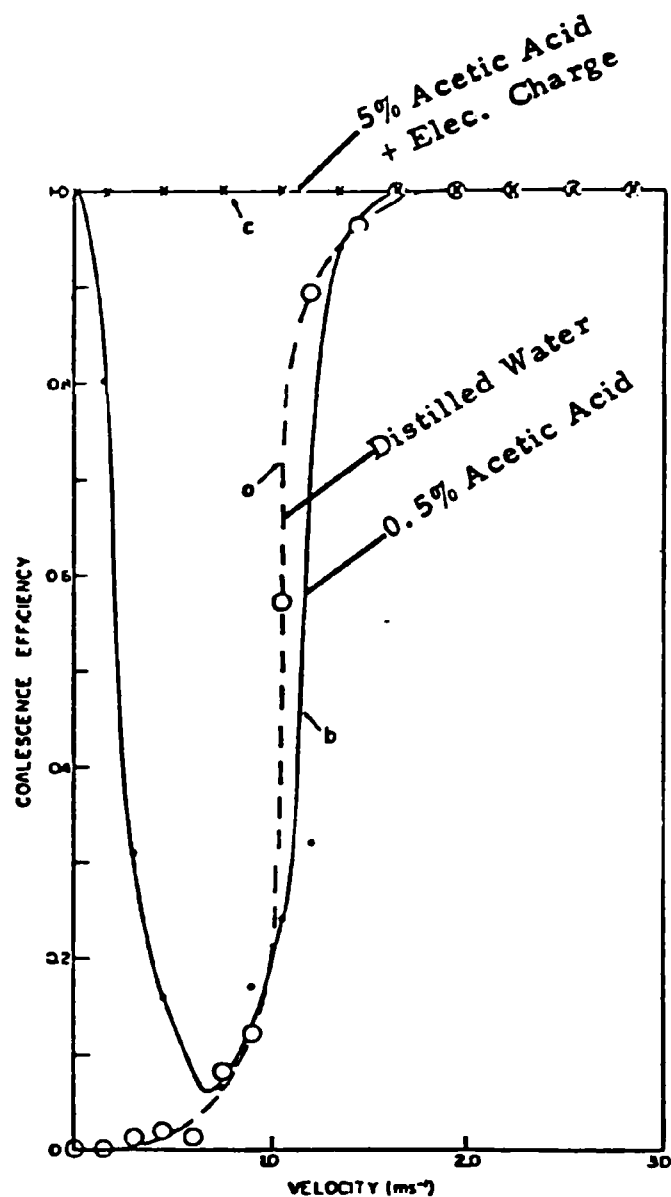
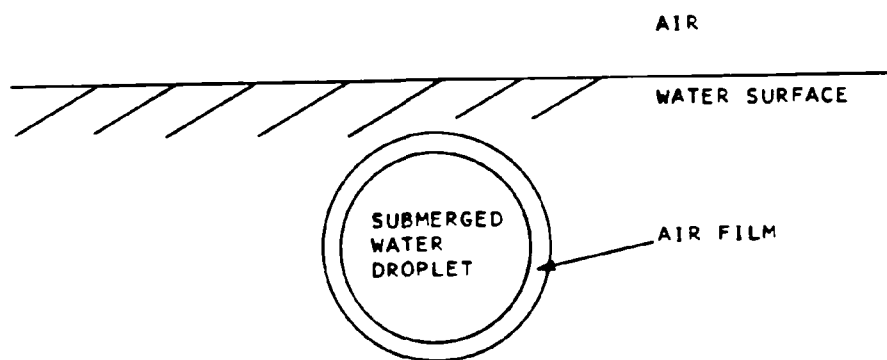


Figure 7. Coalescence efficiency vs velocity of impact of 134μ droplets impinging on 2.2 mm drops: a) distilled water, $\sigma = 77\text{ dyn cm}^{-1}$; b) 0.5% acetic acid solution, $\sigma = 70\text{ dyn cm}^{-1}$; c) 5% acetic acid solution, $\sigma = 60\text{ dyn cm}^{-1}$. Curve c) also resulted for distilled water when the drops were oppositely charged. (List and Whelpdale, 1969)¹²

An inverted bubble is shown in Figure 8. Again it appears that surface forces and surface layers are the dominant mechanism in preventing coalescence. Unfortunately, all of the above effects have been observed with fairly large liquid drops. There is no direct evidence to show whether these phenomena occur between the solid and liquid particles in a scrubber; however, since solid particles are likely to have an adsorbed water film (or other adsorbed films) it seems that surface effects similar to these may occur. Also, it is interesting from a practical viewpoint, that a compound such as acetic acid appears to greatly increase coalescence.



77-341

Figure 8. Inverted bubble

2. The assumptions used to calculate the film thinning model predictions may have been too crude. The Reynolds formula¹⁶ is used to calculate the time, t , for the trapped air layer to thin to a rupture thickness, δ .

$$t = \frac{3}{4} \mu_G \frac{A^2}{\pi F_N} \frac{1}{\delta^2} \quad (10)$$

where A = area of contact
 F_N = force acting on particle normal to surface
 μ_G = absolute viscosity of air
 δ = film rupture thickness

Figure 9 illustrates the important dimensions in the film thinning model.

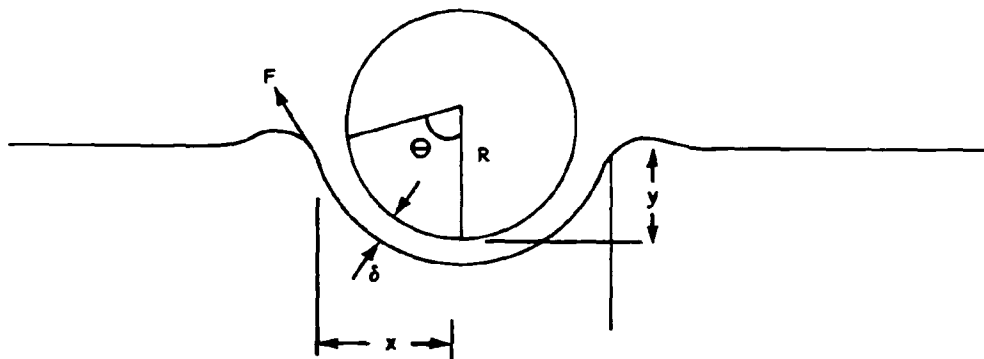


Figure 9. Film thinning model

77-361/1

Equation 10 is valid when $y_{\max} < 0.5 R$, which will include most cases of interest; however, it is also assumed in order to calculate the thinning time, t , that the ratio of F to A^2 is constant. This is simply not the case, in fact, for the models of Lang⁹, Emory¹⁰, and Jayaratne⁵, the ratio of F to A is a constant:

$$F = \gamma A, \quad (11)$$

where γ is a constant depending only on the surface tension and particle radius. Thus the ratio A^2/F must be proportional to A which changes from 0 to A_{\max} (and back to zero if the particle rebounds). Before the particle forms a trapped layer, the area A , is zero and the thinning time, Equation 10, also becomes zero since A^2/F is zero. Thus, the model actually appears to predict that the thinning layer collapses before penetration begins. This conclusion does agree with the data shown in Figure 4 for the 5 percent acid solution. The problem in Equation 10 is that the change of A with respect to F during the collision process has been neglected.

3. Important factors may have been ignored in calculating thinning time. All the calculations discussed above assume that the major forces acting to decelerate the particle result from surface tension. Inertial forces and the droplet internal pressure are neglected. In actuality it is these very forces that are responsible for stopping the particle; the surface tension acts to transmit these forces (to the thinning layer). The surface tension also plays a role in absorbing energy from the incoming particles since the surface stretches. It is likely that the coalescence described by Equation 8 is inaccurate because these forces are neglected. Unfortunately, it is difficult to include inertial effects since the entire process such as the forces acting on the particle through the thinning layer, the thickness of the thinning layer, the flow fields in the droplet, and the form of the depression (not just its relative dimensions) change with time and velocity, and are inter-related. The set of differential equations describing the process and the method of solution are complicated and would require extensive calculations for solution. It is difficult to simplify the processes so that meaningful estimates can be made. Yet, it appears essential that this type of calculation be performed if the film thinning model is to be properly evaluated. The results could easily show that the thinning layer plays a minor part in preventing coalescence.

Another phenomenon which is normally neglected is the stability of the thinning layer. While it does appear likely that a higher surface tension causes the layer to thin more rapidly, increased surface tension will also make the layer more stable. Lang⁹ has given the stability a preliminary treatment but a more detailed study is needed. In particular, it seems intuitively likely that the layer will break down once the thickness at some point approaches the local mean free path. Also, the inertial forces involved in collision are quite large and these too act to decrease stability.

SECTION 6

EXPERIMENTAL EVALUATIONS OF COALESCENCE THEORY

Simple laboratory experiments were devised to measure film thinning times and the effects of surface energy on the thinning times. These experiments were planned to evaluate, at least qualitatively, the film thinning theory.

The impact and coalescence process for a water droplet and a glass sphere (representing a flyash particle) was observed with a high speed motion picture camera looking through a microscope. The water droplets were approximately 1000 to 3000 μm diameter and were suspended on the end of a microliter syringe needle. The glass spheres were made by drawing a glass rod into a fine fiber and forming a ball on the tip end. The particles ranged from 10 to 3500 μm diameter. The suspending rods were as small as 10 μm diameter. Rods 10 μm diameter without a sphere on the end were also used to simulate 10 μm diameter particles.

The experimental setup is shown in Figures 10 and 11. The supporting syringe and glass rod were mounted on three-dimensional micromanipulators so that they could be moved independently within the field-of-view of the camera. The glass particle was caused to impact the water droplet by rapidly advancing the horizontal traverse mechanism of the particle support, Figure 12. Radioactive polonium strips were mounted near the particles and droplets to eliminate electrostatic charges. Radiation from the polonium ionizes the air so that surface charges bleed off. Experiments without the polonium tended to give more variable film thinning time measurements. The camera used was a Beckman and Whitley Dynafax, operating at a top speed of 26,000 frames per second, with individual frame exposure times of 2.5 μsec . The camera is a continuous writing rotating drum camera with 224 frames.

The camera speed was measured to within ± 5 percent. A measurement uncertainty of $\pm 1/2$ frame at each end of the thinning time measurements introduces an additional potential error of $\pm 39 \mu\text{sec}$. A thinning time of 1,000 μsec , therefore, has a random experimental variation of approximately ± 10 percent while a thinning time of 100 μsec , has a random variation of approximately ± 50 percent.

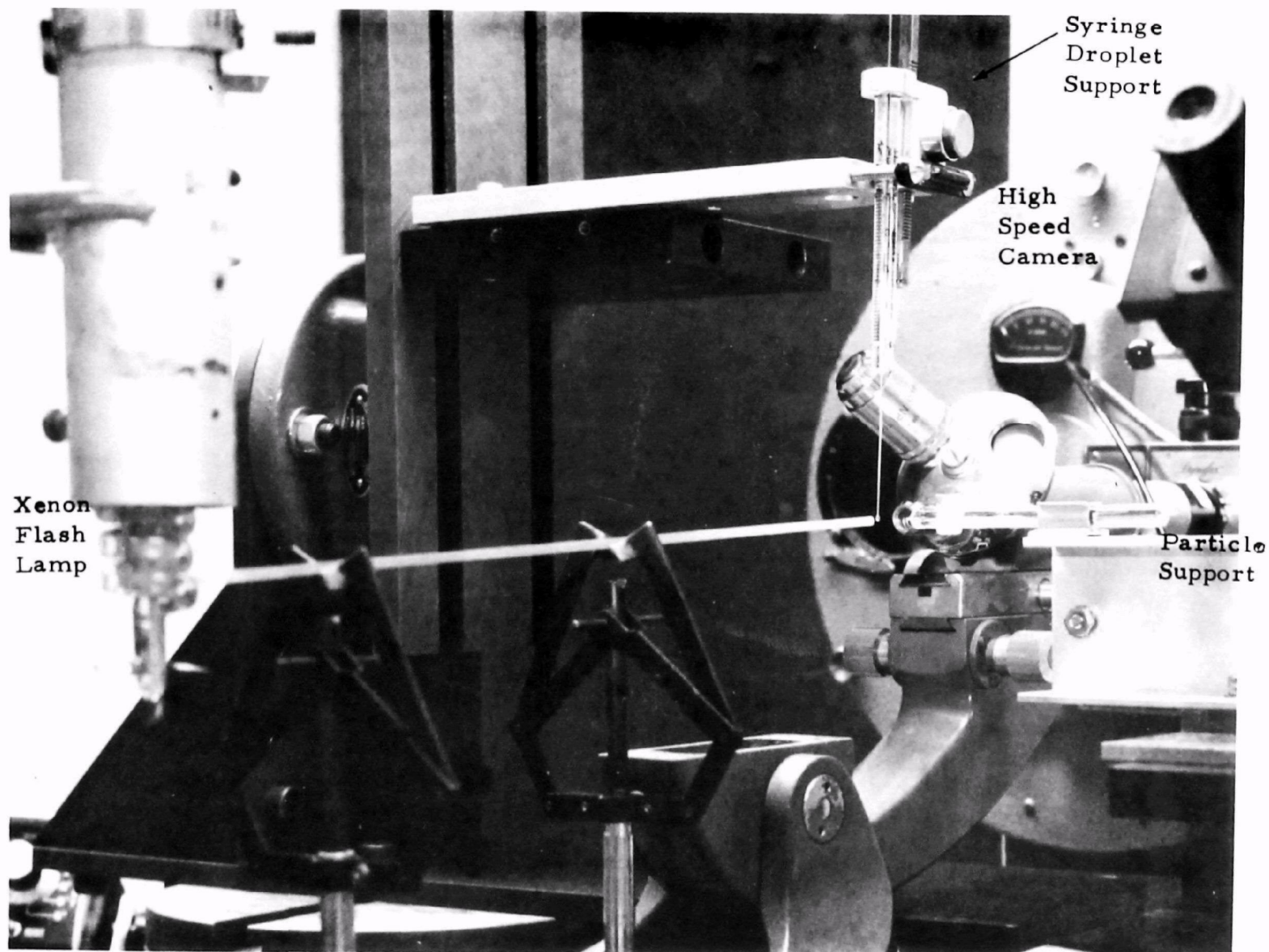
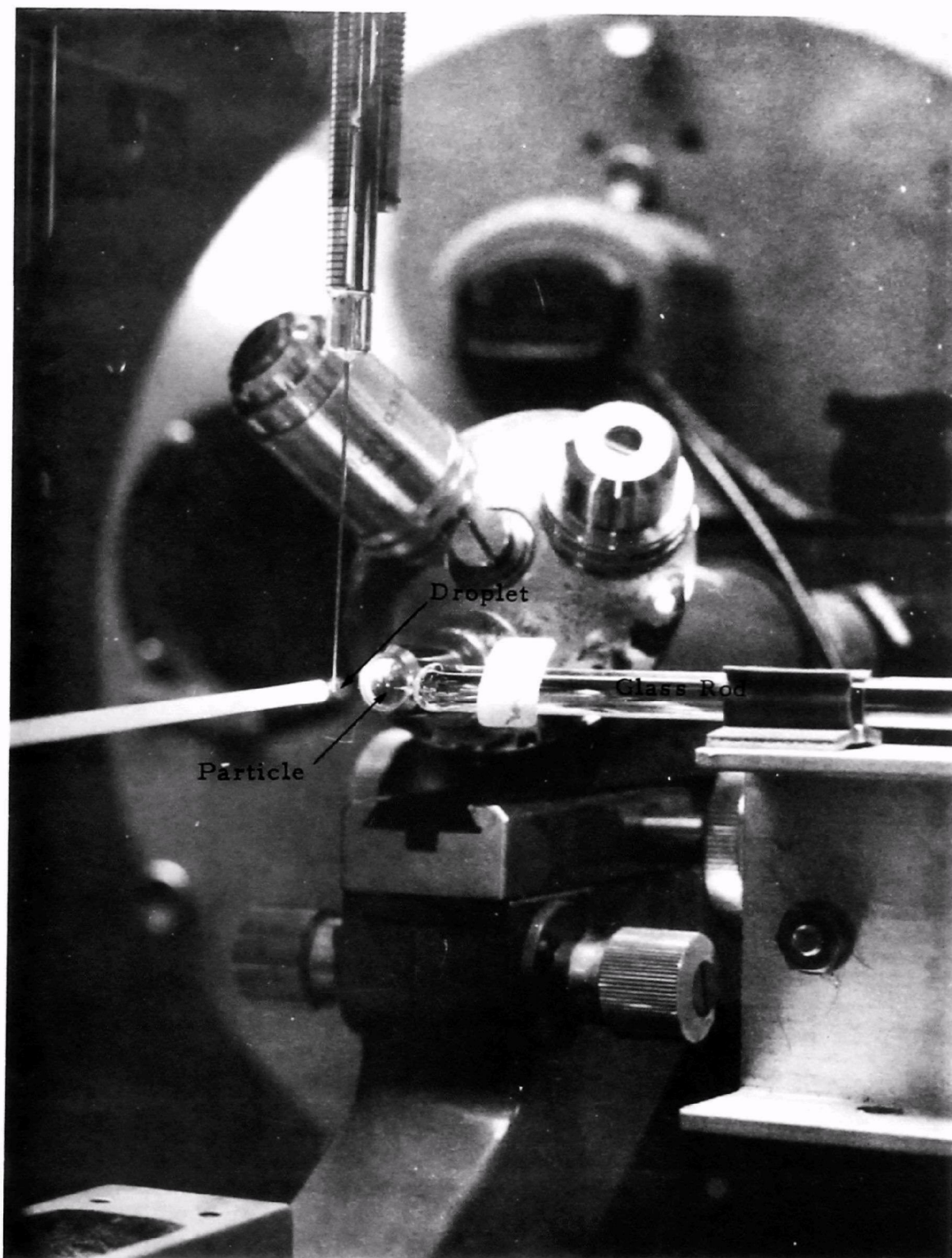


Figure 10. High speed cine microscope equipment used for experimental evaluation of coalescence mechanisms.



77-083

Figure 11. Glass rod with simulated flyash particle mounted on traversing mechanism.



Figure 12. Traversing mechanism for impacting particles into water droplets.

77-114

Coalescence delay times were measured as functions of particle size, impact velocity, and droplet surface tension. Film thinning time was taken as the coalescence delay time; i.e., the time from first contact until a liquid meniscus was first discernable. For example, in Figure 13 first contact occurred on frame 9 and coalescence occurred on frame 24. The delay is therefore equivalent to 15 frames at $39 \mu\text{sec}/\text{frame}$, for a total delay time of $585 \mu\text{sec}$. The time per frame is determined from the camera speed; at 26,000 frames per second the time between frames is $39 \mu\text{sec}$. The camera speed was held constant at 26,000 frames/sec for most of the experiments. A summary of experimental variables is given in Table 2.

TABLE 2. EXPERIMENTAL VARIABLES

Particle Size Range:	10 to 3500 μm diameter
Droplet Diameter:	2 mm, nominal
Droplet Surface Tension:	72 (Distilled Water), 30 (1% Triton X-100 in Water), 17.3 (Freon TF) dynes/cm.
Impact Velocity:	5 to 100 cm/sec.

Typical high speed motion pictures produced during the test program are included in Figures 13 through 25. Table 3 summarizes variables that are illustrated. The cases shown in the figures were selected to show:

1. The decrease in coalescence time resulting from a decrease in particle size (Figures 13 - 18)
2. The minimal change in coalescence delay time resulting from a change in impact velocity (compare Figures 13 - 18 at 6 cm/sec impact velocity with Figures 19 - 25 at 42 cm/sec).
3. The effect of surface tension in reducing coalescence delay times (Figures 23 - 25).

TABLE 3. EXPERIMENTAL VARIABLES ILLUSTRATED IN FIGURES 13-25

<u>Figure No.</u>	<u>Particle Diameter (μm)</u>	<u>Impact Velocity (cm/sec)</u>	<u>Droplet Composition</u>	<u>Surface Tension (Dynes/cm)</u>	<u>Remarks</u>
13	1700	6	Dist. Water	72	No. 13-17 show the effect of changing particle size.
14	1000	6	Dist. Water	72	
15	725	6	Dist. Water	72	
16	275	6	Dist. Water	72	
17	100	6	Dist. Water	72	
18	10	42	Dist. Water	72	No. 19-25 are replicate experiments to demonstrate reproducibility.
19	275	42	Dist. Water	72	
20	275	42	Dist. Water	72	
21	275	42	Dist. Water	72	
22	275	42	Dist. Water	72	
23	100	42	Freon TF	17.3	Homogeneous low surface tension droplets.
24	100	42	1% X-100 in Dist. Water	30	Surfactant, low surface tension water droplets
25	100	42	Dist. Water	72	Distilled water for comparison with Figure 24.

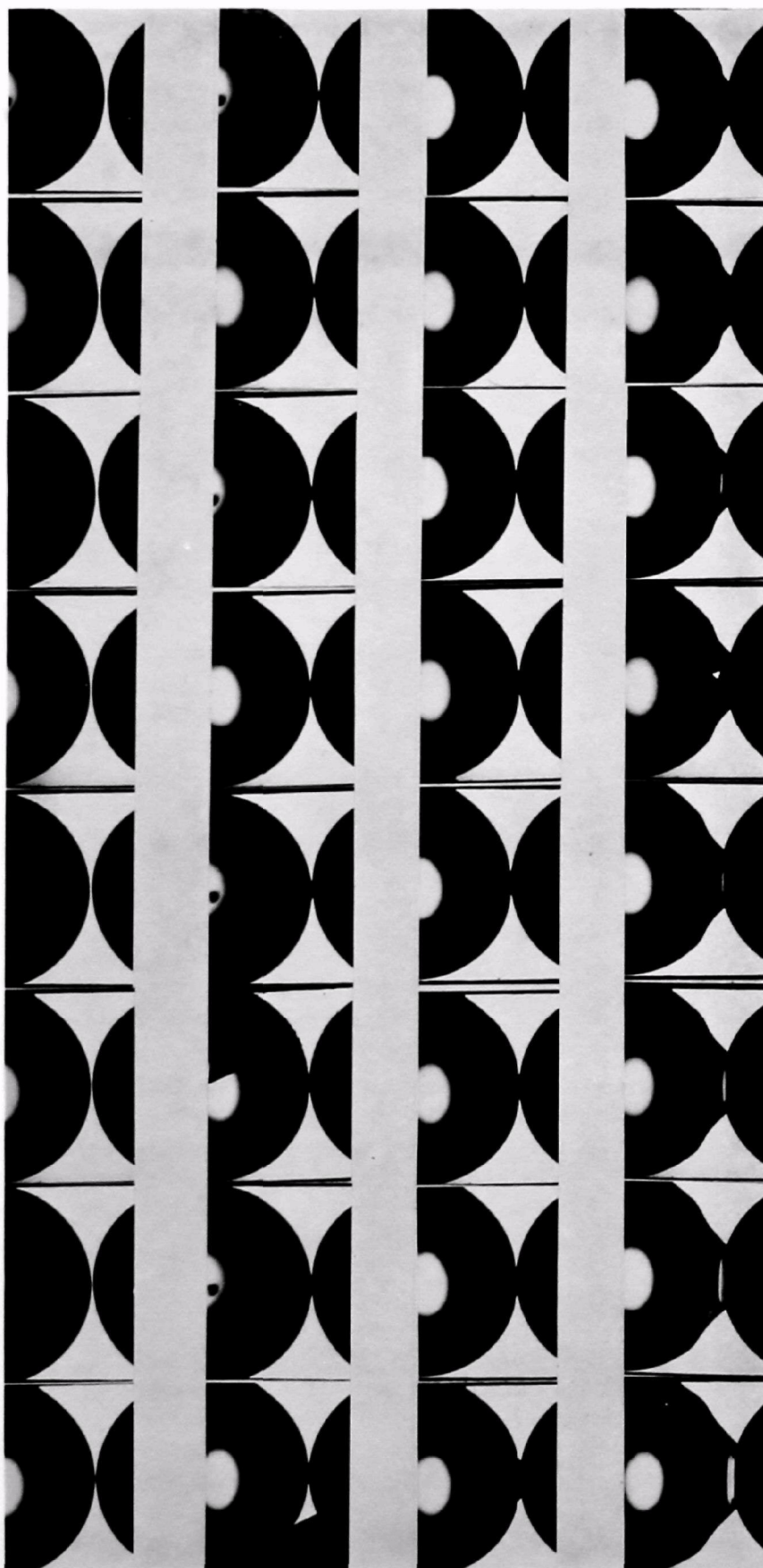


Figure 13. Coalescence of 1700 μm diameter glass particle with water droplet, 585 μsec delay, 6 cm/sec.

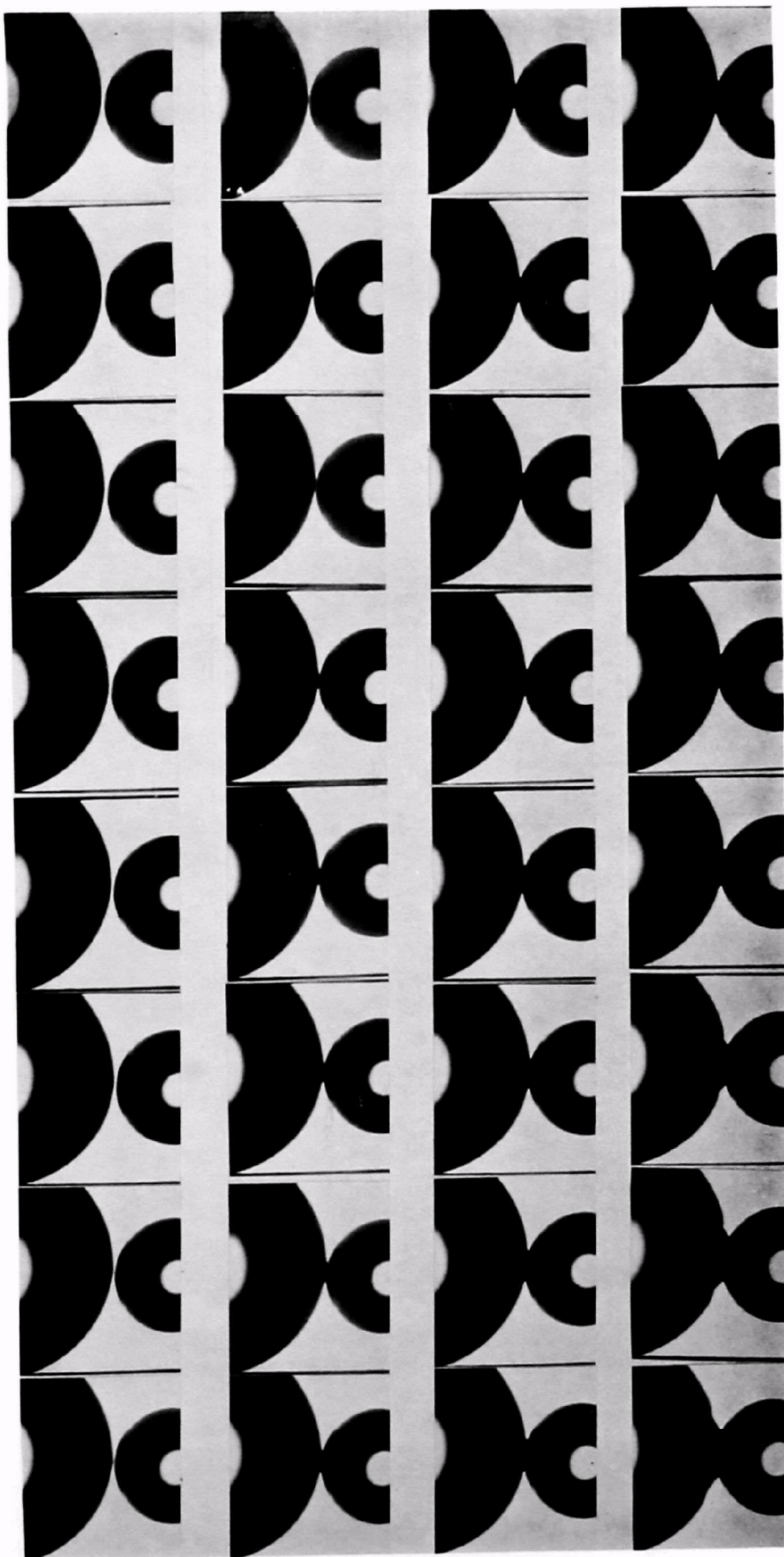
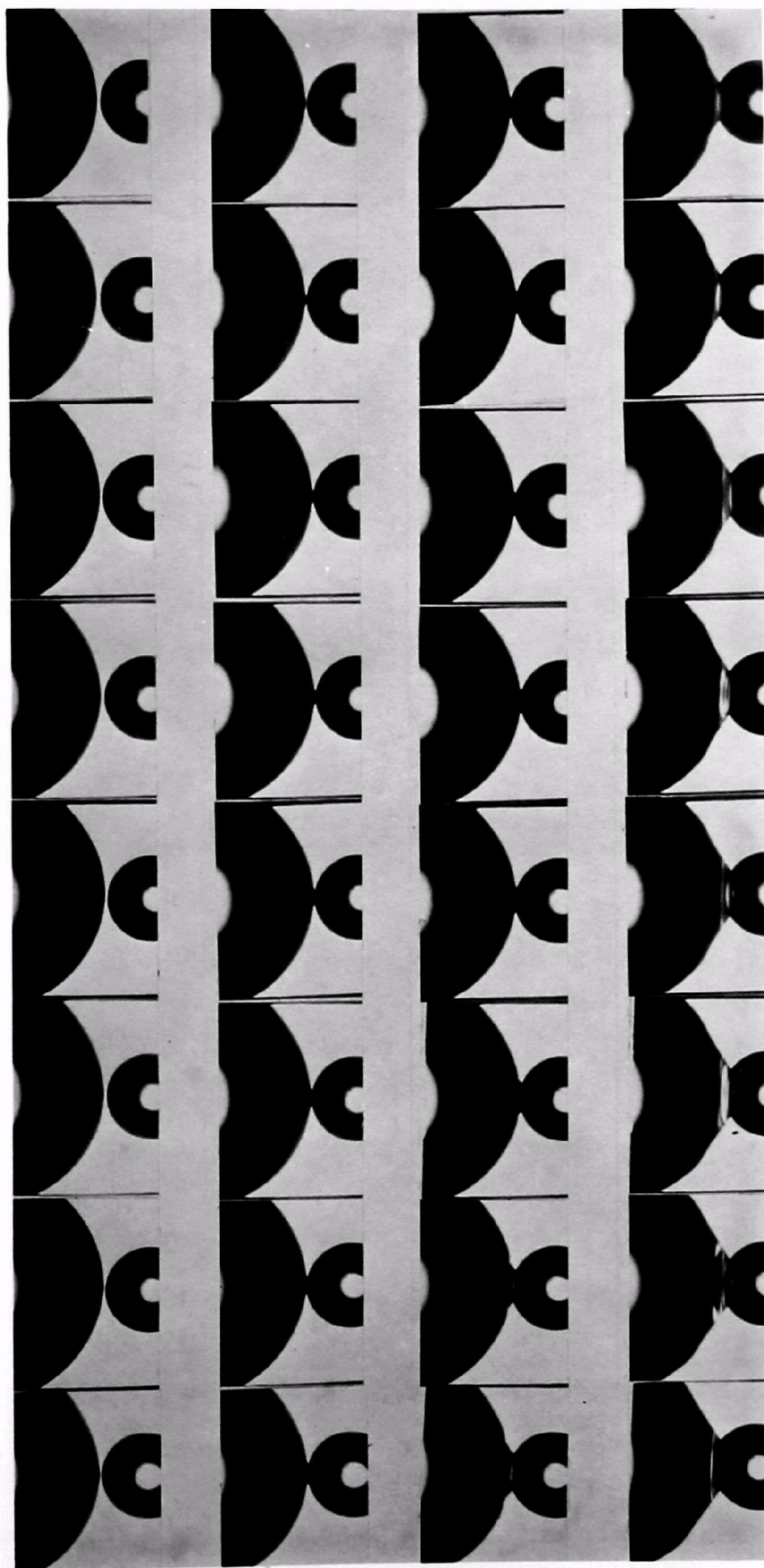


Figure 14. Coalescence of 1000 μm diameter glass particle with water droplet, 780 μsec delay, 6 cm/sec.



77-120

Figure 15. Coalescence of 725 μm diameter glass particle with water droplet, 468 μsec delay, 6 cm/sec.

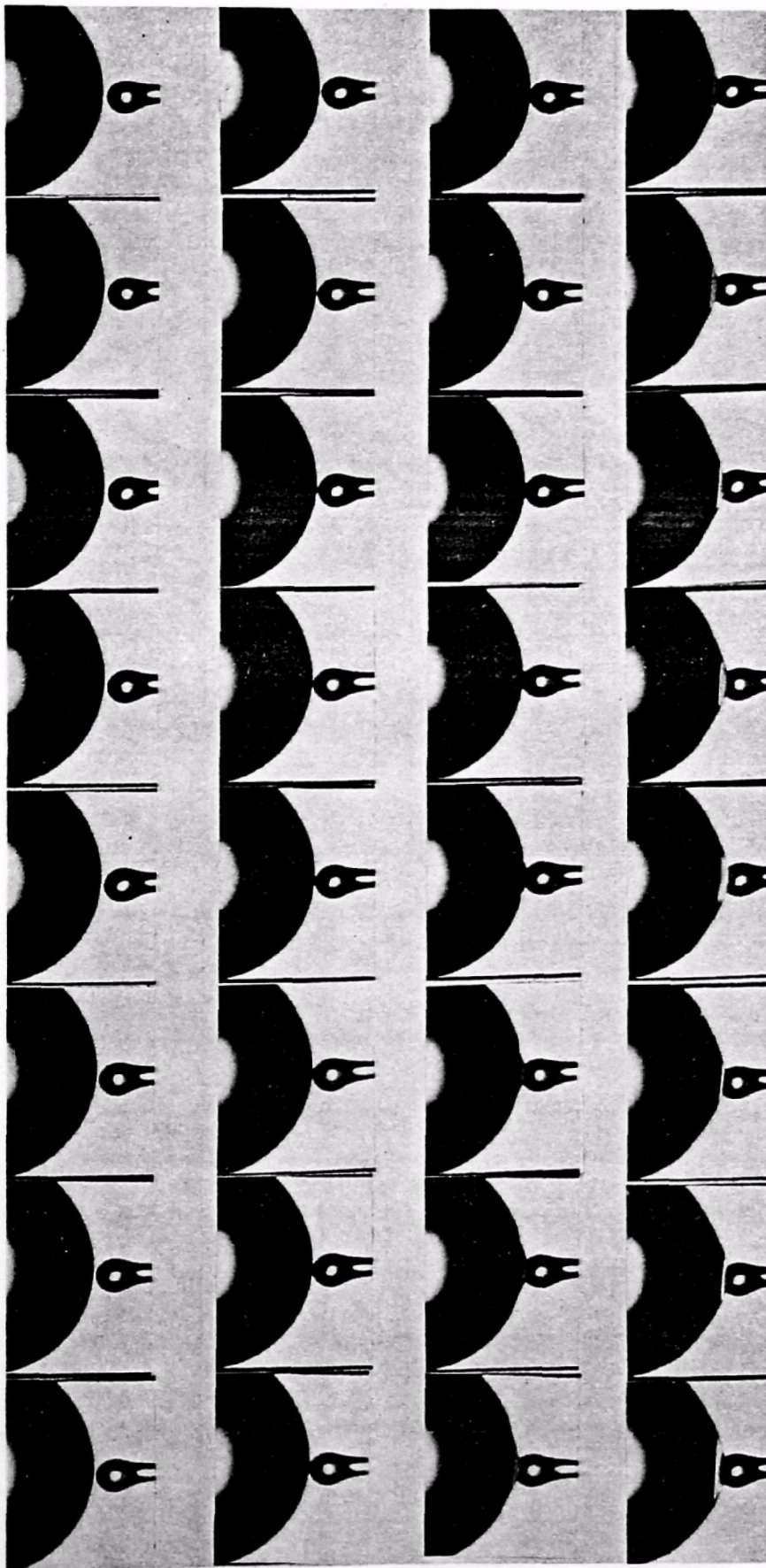


Figure 16. Coalescence of $275\text{ }\mu\text{m}$ diameter glass particle with water droplet, $351\text{ }\mu\text{sec}$ delay, 6 cm/sec .

77-121

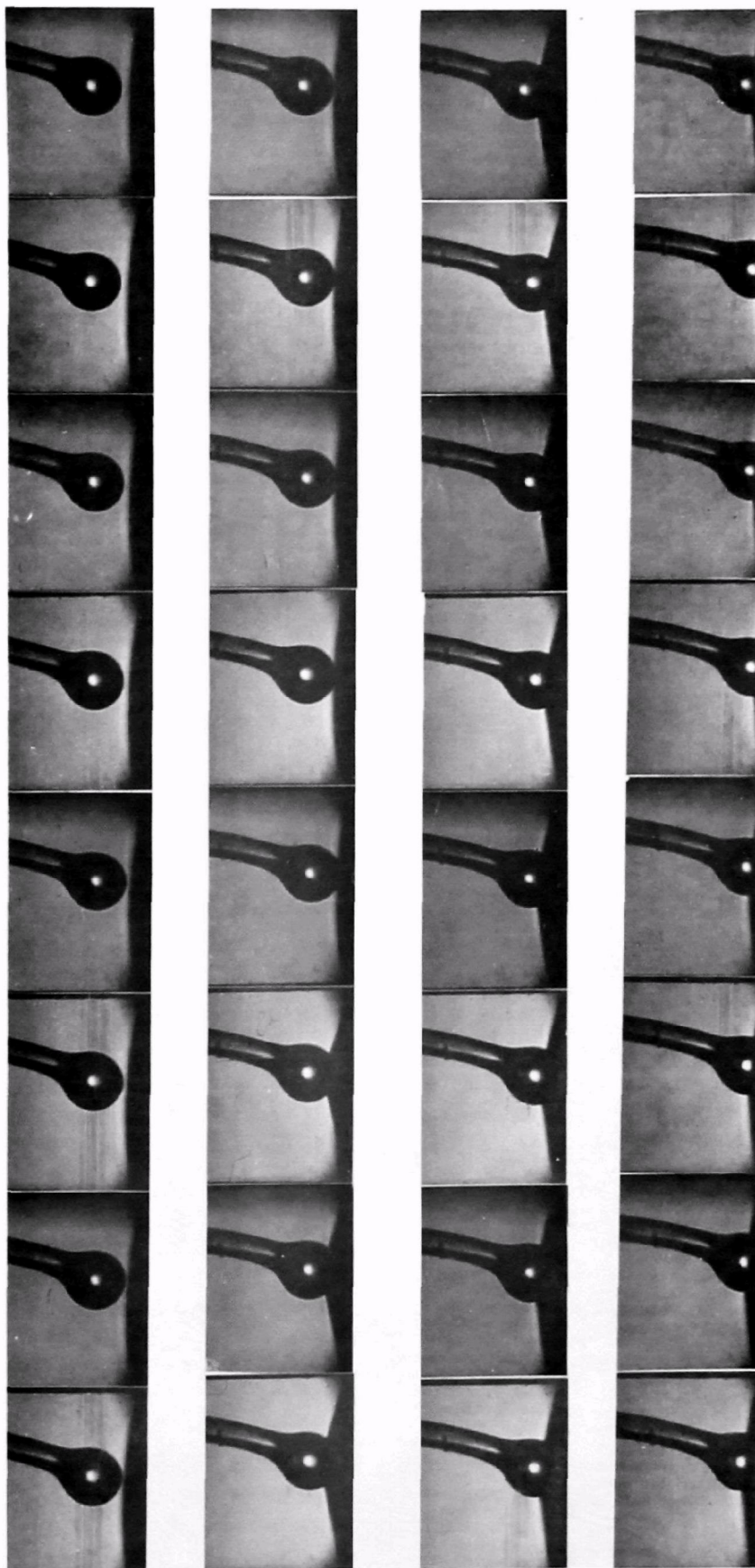
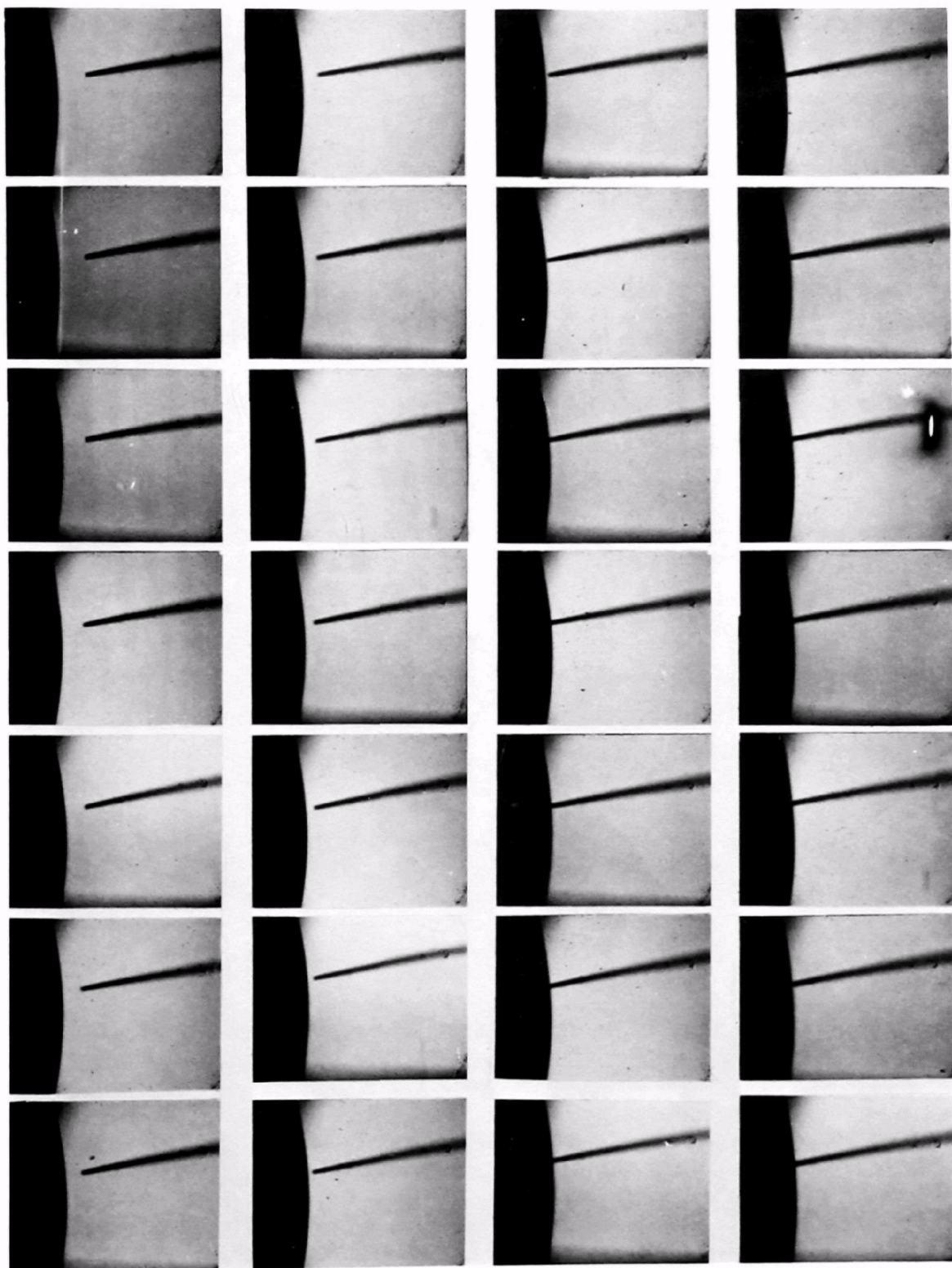


Figure 17. Coalescence of 100 μm diameter glass particle with water droplet, 156 μsec delay, 6 cm/sec.

77-122



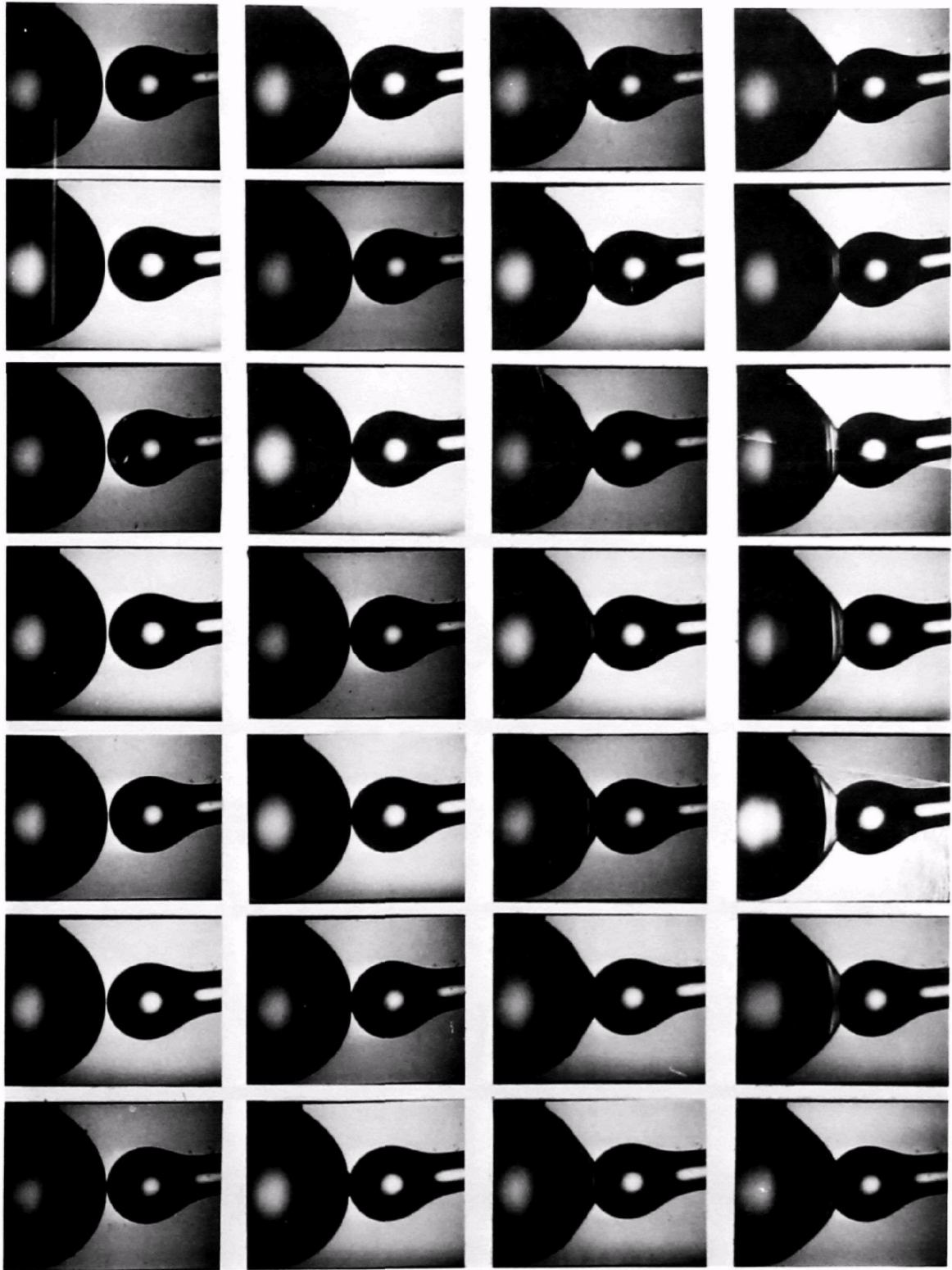
77-350

Figure 18. 10 μm diameter glass fiber impacting distilled water droplet. Coalescence delay time < 1 frame (i.e., $< 39 \mu\text{sec}$).



77-351

Figure 19. Coalescence of 725 μm diameter glass particle
with water droplet, 273 μsec delay, 42 cm/sec.



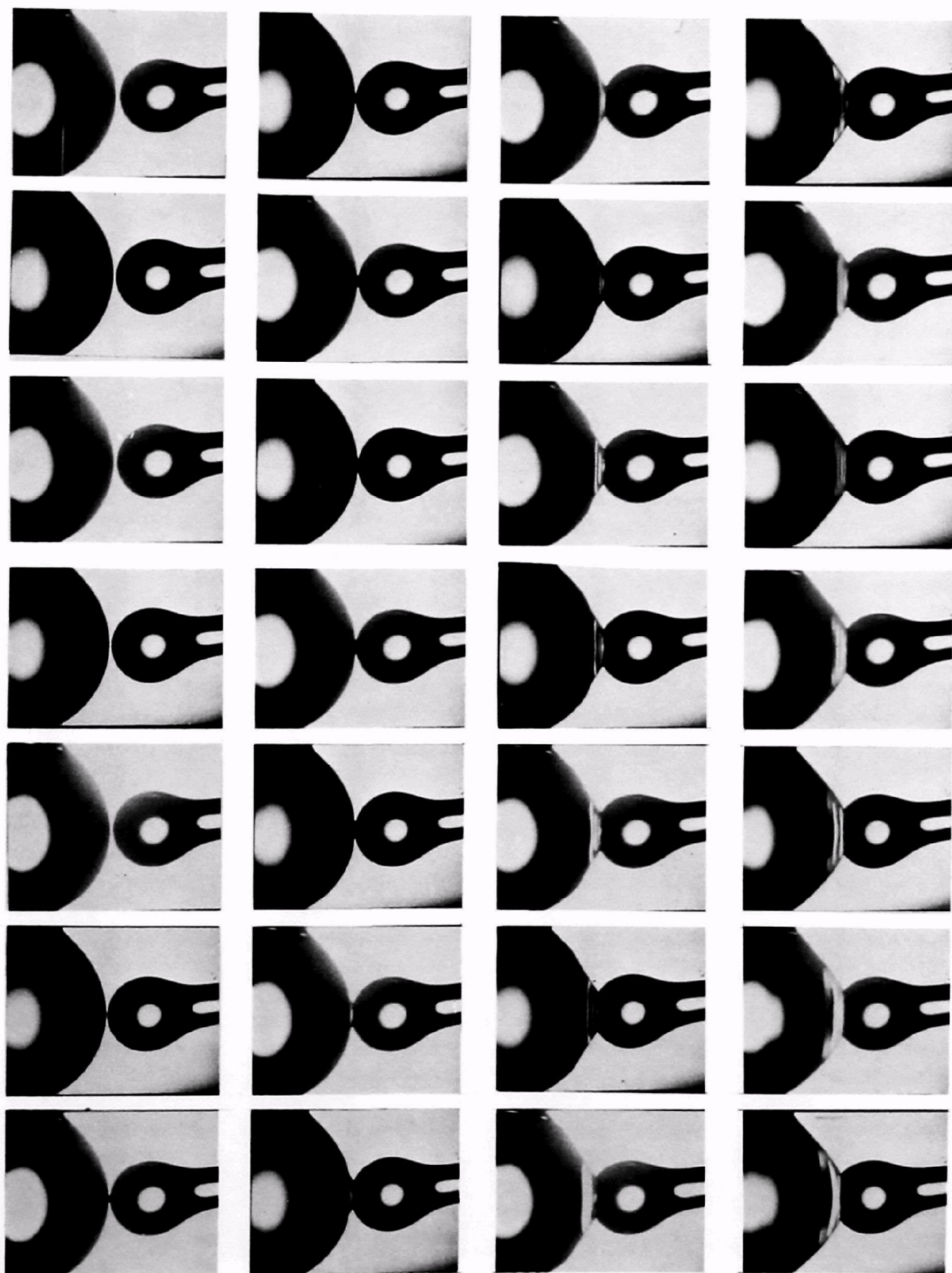
77-345

Figure 20. Coalescence of 725 μm diameter glass particle with water droplet, 234 μsec delay, 42 cm/sec.



77-342

Figure 21. Coalescence of 725 μm diameter glass particle with water droplet, 273 μsec delay, 42 cm/sec.



77-347

Figure 22. Coalescence of 725 μm diameter glass particle with water droplet, 234 μsec delay, 42 cm/sec.

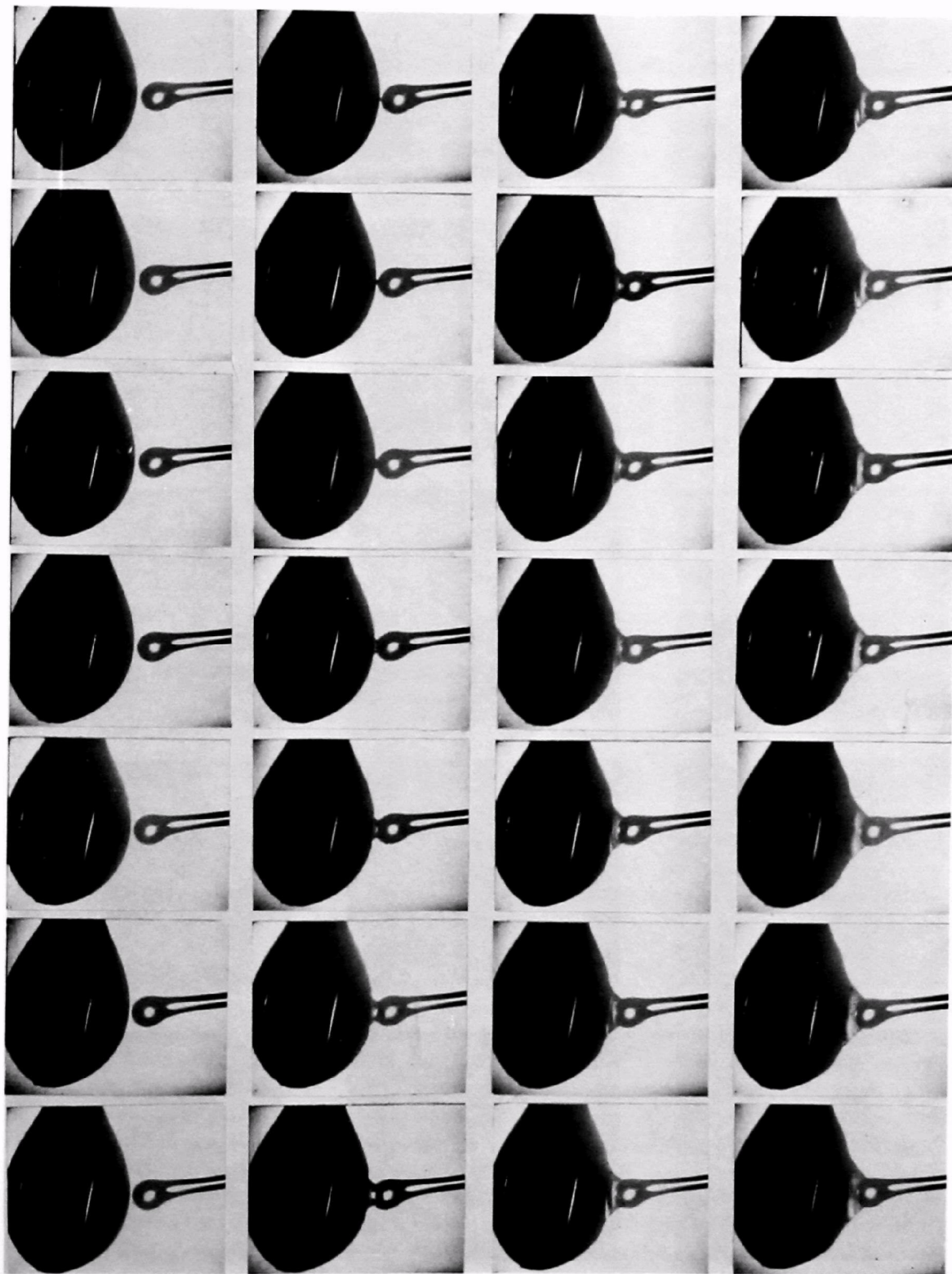
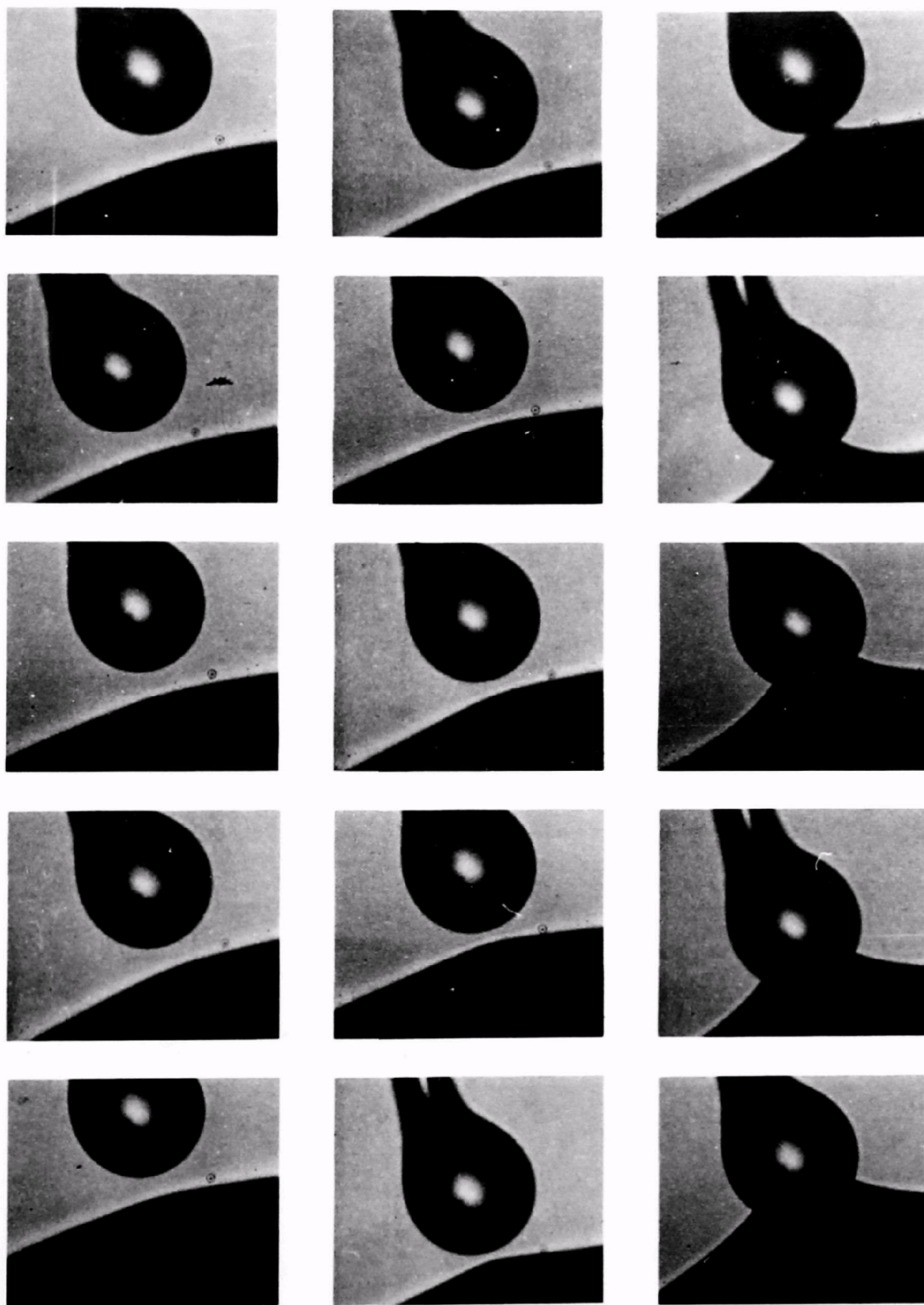
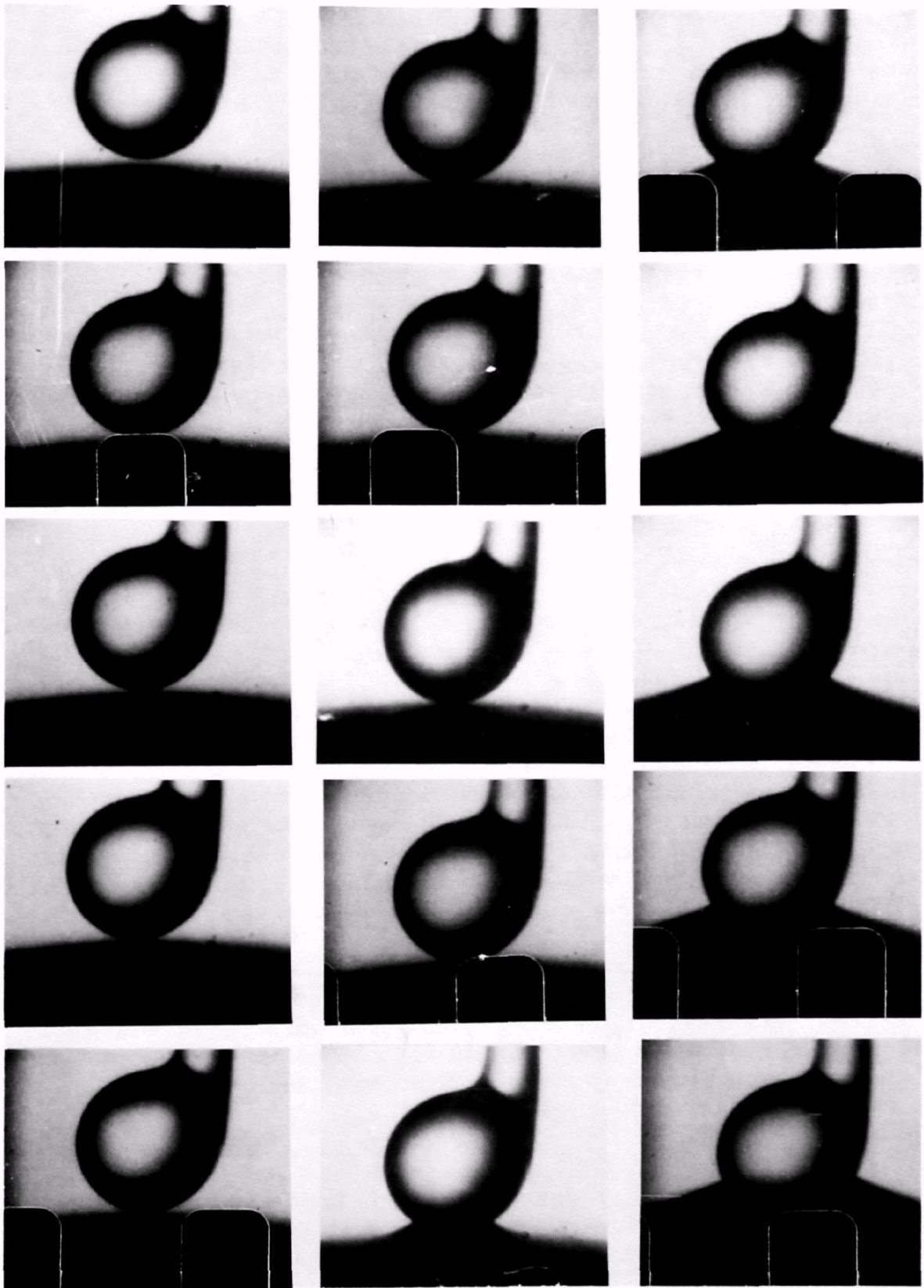


Figure 23. Coalescence of 100 μm diameter glass particle with Freon TF, $< 39 \mu\text{sec}$ delay, 42 cm/sec. 77-348



77-081

Figure 24. Coalescence of 100 μm diameter glass particle with water/surfactant, $< 39 \mu\text{sec}$ delay, 42 cm/sec.



77-076

Figure 25. Coalescence of 100 μm diameter glass particle with water droplet, 156 μsec delay, 42 cm/sec.

Delay time measurements for water droplets with an impact velocity of 6 cm/sec are plotted as a function of particle diameter in Figure 26 for comparison with theoretical predictions from the film thinning model of Emory¹⁰.

The experimental results are consistent and reasonably reproducible; however, they differ from the theoretical predictions by as much as 2 orders of magnitude for larger droplets. For the large particle experiments, the particles were nearly the same size as the water droplets. An error could, therefore, be introduced by the false assumption that the droplet was large compared to the solid particle. Some of the random experimental variation could also be due to uncontrolled parameters including ambient temperature, relative humidity, water purity, and particle cleanliness. No special control of these factors was made; however, because of the limited ranges of variations they are not expected to have large effects. Ambient temperatures ranged from 19 to 22° C (67 - 72° F). Relative humidity ranged from 40 to 50 percent.

Figure 27 shows the results obtained when the velocity was increased to 43 cm/sec. The dotted lines showing the range of scatter for the 6 cm/sec velocity data are included for comparison. It appears that delay times are slightly shorter at the higher velocity, especially for small particles.

The high velocity results were repeated using droplets of Freon-TF instead of water. The Freon represents a homogeneous liquid with a low surface tension, approximately 17.3 dynes/cm, (compared to 72 dynes/cm for pure water). A homogeneous liquid was selected in order to minimize the effect of the polarized Helmholtz double layer that is expected to be present at the surface of water droplets containing a surfactant. The short range molecular dipole forces in the double layer could have an effect on coalescence that is separate from the surface tension effect by itself.

Results of the Freon coalescence measurements are given in Figure 28. It appears that the range of random variation in the measurements is wider than for the water droplet coalescence measurements. None of the Freon-TF delay times were longer than for water but some were considerably shorter. Therefore, if there is an effect on a delay time due to the reduced surface tension of Freon-TF, the effect appears to reduce the delay time.

Results of experiments using surfactants in water are given in Figure 29. There is insufficient data available to draw conclusions at this time, however, it appears that if there is an effect on coalescence delay time due to addition of a surfactant, the delay is shorter.

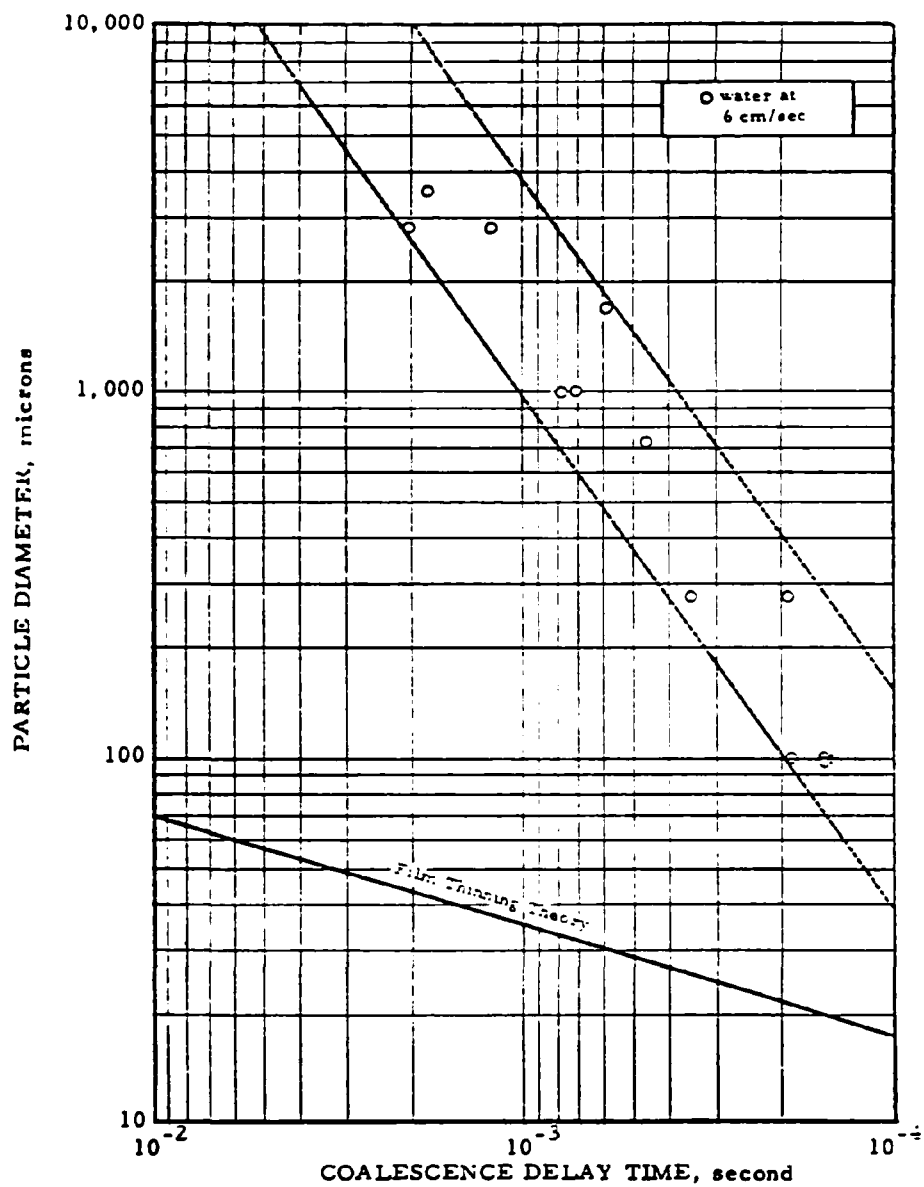


Figure 26. Comparison of theoretical predictions and experimental measurements of coalescence delay time for water at 6 cm/sec impact velocity.

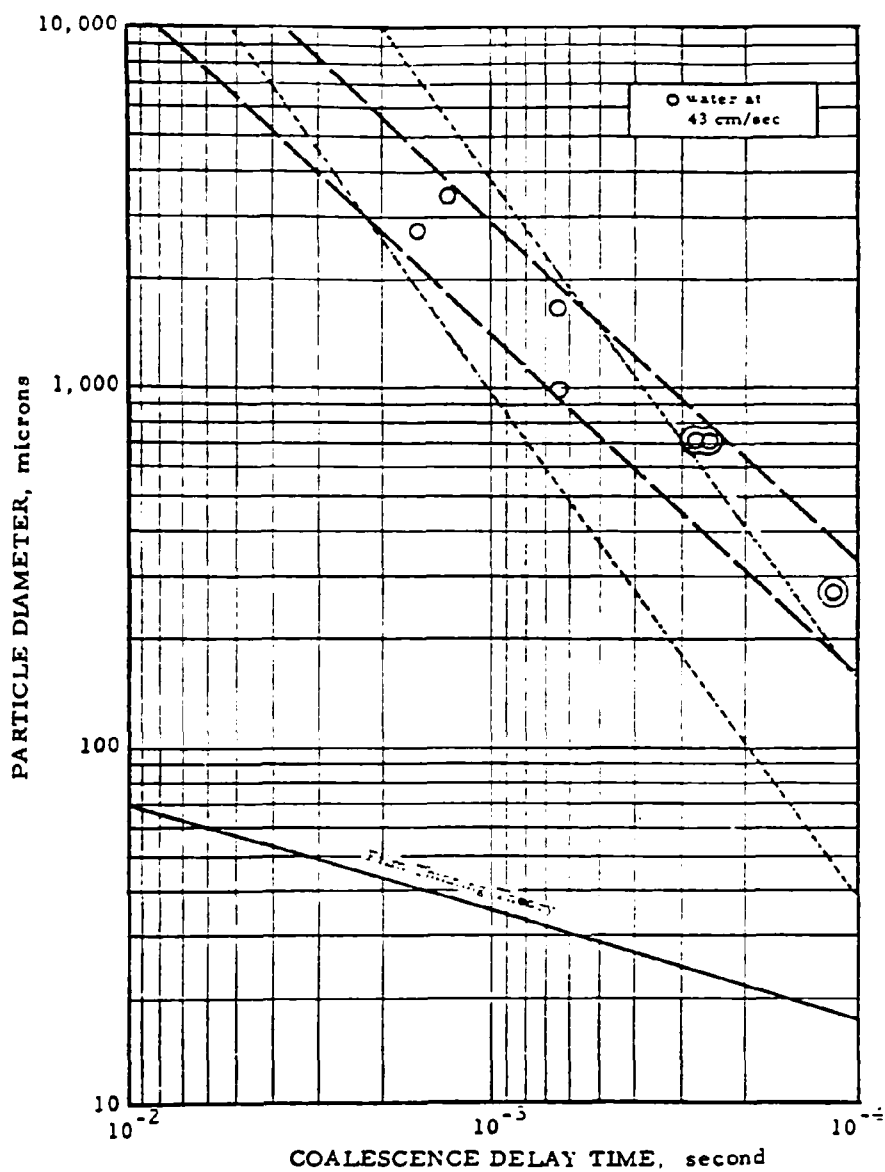
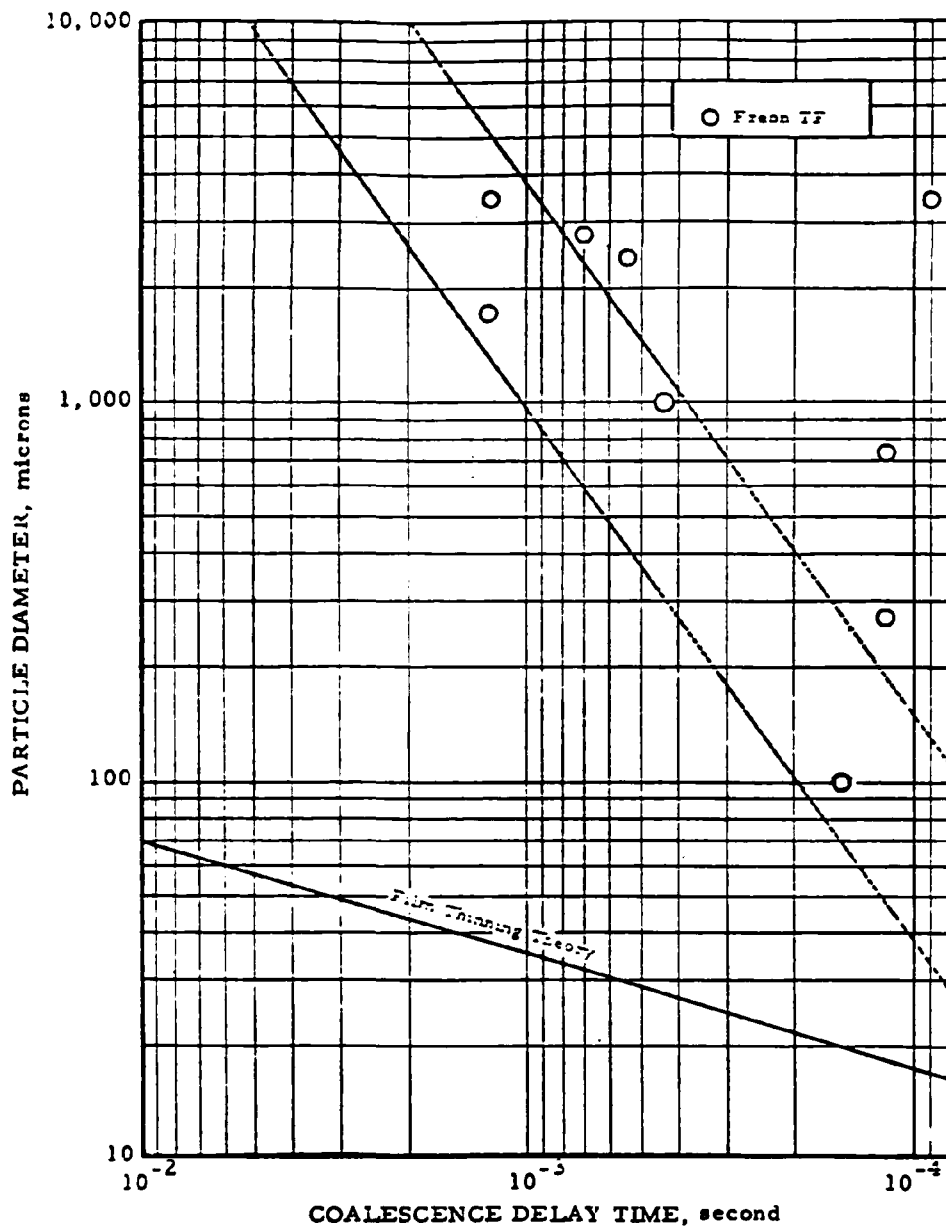


Figure 27. Comparison of theoretical predictions and experimental measurements of coalescence delay time for water at 43 cm/sec impact velocity.



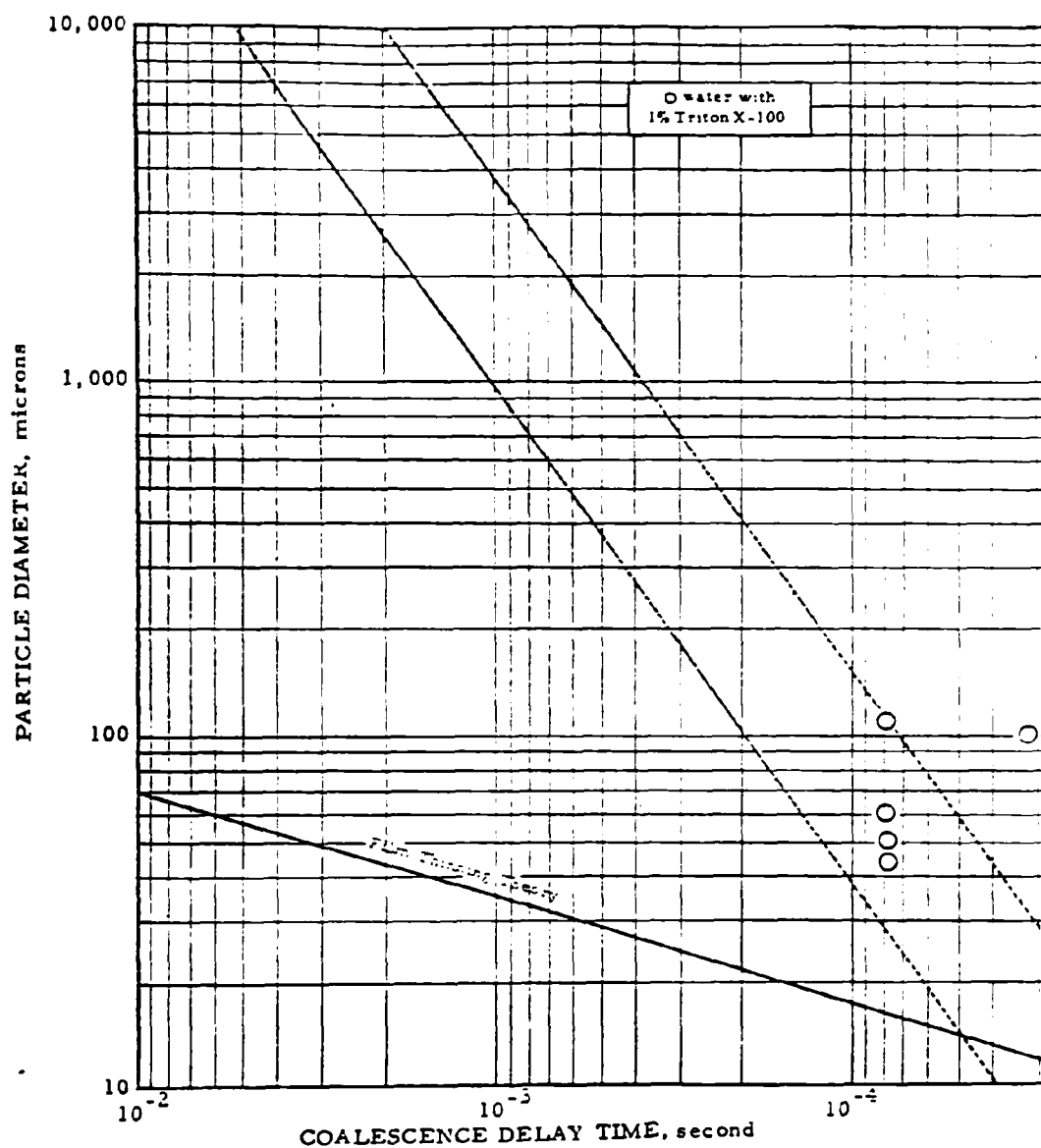


Figure 29. Comparison of theoretical predictions and experimental measurements of coalescence delay time for water droplets containing surfactant and an impact velocity of 42 cm/sec.

REFERENCES

1. Calvert, S., Yung, S., Barbarika, H., Venturi Scrubber Performance Model. Air Pollution Technology, Inc., Final Report to U. S. Environmental Protection Agency, Research Triangle Park, North Carolina, 1976. 196 pp.
2. Bughdadi, S. M., Effect of Surfactants on Venturi Scrubber Particle Collection Efficiency, M. S. Thesis. Department of Thermal and Environmental Engineering, Southern Illinois University of Carbondale, 1973.
3. Nuykiyama, S., and Tanasawa, Y., Trans. Soc. Mech. Eng. (Japan) 4, 86, 138 (1938); 5, 62, 68 (1939); 6, II-7 II-15 (1939); 6, II-18 (1940).
4. Wolfe, H. E., and Andersen, W. H., Kinetics, Mechanism, and Resultant Droplet Sizes of the Aerodynamic Breakup of Liquid Drops. Aerojet-General Corporation Report No. 0395-04 (18) SP, 1964.
5. Jayaratne, O. W., and Mason, B. J., The Coalescence and Bouncing of Water Drops at an Air/Water Interface. Proc. Roy. Soc., A(280): 545, 1964.
6. Schotland, R. M., Experimental Measurements Relating to the Coalescence of Water Drops with Water Surfaces. Disc. Faraday Soc., (30): 72, 1960.
7. Lobl, E. L. personal communication, 1976.
8. Levin, Z., Neiburger, M., and Rodriguez, L., Experimental Evaluation of Collection and Coalescence Effects in Cloud Drops. J. Atmos. Sci., 30(1): 944-946, 1973.
9. Lang, S. B., and Wilke, C. R., A Hydrodynamic Mechanism for the Coalescence of Liquid Drops. University of California, Berkeley, California, 1971. 23 pp.

10. Emory, S., and Berg, J., The Effect of Liquid Surface Tension on Solid Particle-Liquid Droplet Coalescence. University of Washington, Task Report to U. S. Environmental Protection Agency, Contract No. 68-02-2109. May, 1977.
11. Arbel, N., and Levin, Z., The Coalescence of Water Drops, I. A Theoretical Model of Approaching Drops, and II. The Coalescence Problem and Coalescence Efficiency. Department of Geophysics and Planetary Sciences, Tel Aviv University, Ramat Aviv, Israel, 1977. I. 25 pp. II. 25 pp.
12. List, R., and Whelpdale, D. M., A Preliminary Investigation of Factors Affecting the Coalescence of Colliding Water Drops. J. Atmos. Sci., (26): 305, 1969.
13. Stong, C. L., Water Droplets That Float on Water, and Lissajous Figures Made with a Pendulum. Scientific American, August, 1973. pp. 104-109.
14. Stong, C. L., Curious Bubbles in Which a Gas Encloses a Liquid Instead of the Other Way Around. Scientific American, April, 1974. pp. 116-121.
15. Reynolds, O., Phil. Trans. Roy. Soc., A(177):157 1886.

APPENDIX

SURFACE TENSION EFFECTS ON PARTICLE COLLECTION EFFICIENCY

By

Scott F. Emory and

John C. Berg

Department of Chemical Engineering
University of Washington
Seattle, WA 98195

ABSTRACT

Modifications in existing theory concerning the collection on non-wettable or partially non-wettable particles in wet scrubbers are presented. In particular, the requirement for the thinning and rupture of a gas film between particle and liquid is included. Results suggest that decreasing the liquid surface tension may decrease the probability of particle capture.

Introduction

The commonly used models for the wet scrubbing of particulates from gases assume that collision of the solid particles with the surface of the scrubbing liquid always results in the capture of the particles (Goldshmid & Calvert, 1963). Such a view seems to be supported indirectly by the general success of predictions based on that assumption, of overall collection efficiency of scrubbers removing a wide variety of particulates.

Nonetheless, the formal possibility of collision efficiencies less than 100% was acknowledged by Fuchs (1964), and seemingly valid reasons were advanced for supposing that all collisions should not necessarily result in attachment. In particular it was believed that non-wettable particles might simply be reflected if they did not penetrate the liquid to sufficient depth to allow total envelopment. Pemberton (1960) developed predictions of collection efficiencies for totally non-wettable particles (contact angle = 180°) based on the above envelopment criterion, and McDonald (1963) later extended the model to cases of partial non-wettability ($90^{\circ} < \text{contact angle} < 180^{\circ}$). The Pemberton-McDonald model implied that for given solid particles the capture fraction, and hence the collection efficiency, should increase if the surface tension of the collecting liquid is reduced. The use of surface active agents might thus be advantageous in improving collection efficiency, and indeed some reported results suggest that this is the case (Hesketh, 1974; Rabel, 1965). Such increases in overall collection efficiency might also be explained, however, by a greater degree of atomization of the collecting liquid. Other results (Taubman & Nikitina, 1956, 1957; Drees, 1966; Goldshmid & Calvert, 1963) suggest, moreover, that just the opposite occurs, i.e., collection efficiency falls when

the liquid surface tension is reduced. Still other reports (Weber, 1968, 1969) claim no effect at all. In an attempt to resolve some of the above apparent contradictions, and in particular to assess the findings of adverse effects of surfactant, the present work re-examines the assumptions and development of the Pemberton-McDonald theory.

Improved Model

Two significant shortcomings of the Pemberton-McDonald theory are that:

- 1) No allowance for the thinning of the vapor film between the solid particle and liquid surface is made i.e., the film is assumed to rupture immediately upon "impact", and
- 2) Rebouncing particles, i.e, particles without sufficient kinetic energy to produce total envelopment are thought to escape even though coalescence has been assumed.

A more plausible sequence leading to particle capture is as follows.

Initially at least, a particle deforms the liquid surface inward while nested in a thinning but unruptured vapor film. Short of complete envelopment, the particle is caught if coalescence, i.e., vapor film rupture, occurs before the particle comes to rest and rebounds. After coalescence, wettable particles would reside in the droplet interior and non-wettable particles, rather than escaping, would be retained in the liquid surface by surface tension forces acting as dictated by small receding contact angles. This new view is strongly supported by the work of Weber (1968, 1969) who observed experimentally that reduction in particle wettability did affect the location of the captured particle but did not prevent capture itself, which occurred every time actual contact was observed between liquid and particle. Thus an appropriate criterion for capture, in contrast to that of complete

envelopment, is that the vapor film thinning proceed fast enough for coalescence to occur during the particle penetration/rebound cycle. All particles except those corresponding to the limit of total non-wetting should be equally capable of capture regardless of their specific wettability, provided only that the particle/liquid interaction time is greater than the time required for the vapor film thinning. Predicted trends in capture efficiency with fluid properties and system parameters should thus reflect the trends predicted for the ratio of interaction time to film thinning time, R . Large values of this ratio assure capture while values much less than unity indicate no capture. Present knowledge of the details of the film thinning process in particular is not adequate to permit quantitative evaluation of the above ratio, but qualitative predictions of its trends with such parameters as liquid surface tension, particle size and particle velocity (relative to the liquid) should be possible if other factors are assumed to remain unchanged.

The objective of the computations which follow is the prediction of such qualitative trends, and while the models used for calculating both the particle/liquid interaction time and the film thinning time are highly simplified, we believe them to reflect the important features of both processes.

An approximate solution for the particle/liquid interaction time can be obtained by considering the vapor and liquid phases separately and assuming the liquid surface at any instant to have the easily-described shape shown in Figure 1. The particle is thus modelled as a smooth sphere nested in a vapor film of uniform thickness. The liquid surface is initially flat, a good assumption since the collecting droplets are usually more than a thousand times larger than the particles. We assume further that the total force resisting deformation of the liquid surface is the sum of a

surface tension and a viscous contribution so that the equation of motion for the particle becomes:

$$M_p \frac{d^2 Z}{dt^2} = - (F_\sigma + F_\mu) \quad , \quad (1)$$

with initial conditions ($t = 0$): $Z = -R$ and $dZ/dt = V_0$. Inertial effects in the liquid are thus neglected. Neither Brownian motion nor slip between the particle surface and the gas are considered so that the present treatment is restricted to particle sizes larger than approximately $0.5 \mu\text{m}$.

Referring to Figure 1, we write for the surface tension force resisting particle entry:

$$F_\sigma = 2\pi\sigma R \sin^2 \theta \quad (20)$$

The viscous resistance to deformation will be a form drag only, ignoring the viscosity of the thinning film in the computation of particle/liquid interaction time. We assume provisionally that the drag experienced by the vapor-enveloped penetrating particle can be approximated as the appropriate portion of the drag on a completely submerged bubble moving with the same velocity through an infinite medium in pseudo-steady creeping flow. For this case, the pressure profile is (Levich, 1962):

$$p_r = -\mu \frac{VR}{r^2} \cos \theta, \quad (3)$$

from which

$$F_\mu = \frac{2}{3} \pi \mu R V \left[\left(\frac{Z}{R} \right)^3 + 1 \right] \quad , \quad (4)$$

It is found that for all reasonable values of the system parameters, F_μ is at least three orders of magnitude less than F_σ . It thus appears to contribute negligibly to the total force resisting particle entry, and refinements in the computation of its value are unwarranted.

The rate of thinning of a spherical film of vapor (air) has been given by Lang (1962) in the form:

$$\frac{dh}{dt} = \frac{-Fh^3}{24\pi R^4 \mu_{\text{air}} P(\theta)} \quad , \quad (5)$$

where $P(\theta) = \cos(\pi-\theta) - 1 - 4 \ln [\cos(\frac{\pi-\theta}{2})]$. The compressive force, F , in Equation (5) is equal at any instant to the total force resisting penetration, viz., $F_\sigma + F_\mu \approx F_\sigma$. An estimate of the time for thinning to rupture can be obtained by assuming that the rupture thickness, H , is very much smaller than the initial thickness and that the compressive force is constant with time and equal to the average penetration resistive force. We can then write for the thinning time:

$$t = \frac{12\pi R^4 \mu_{\text{air}}}{\bar{F}_\sigma} P(\theta) \frac{1}{H^2} \quad . \quad (6)$$

In order to obtain numerical estimates of t , we assume further that rupture occurs at a film thickness of 50\AA [Ewers and Sutherland (1952) predict that molecular fluctuations will guarantee rupture at this film thickness.] and that the angle θ used in the calculation corresponds to the point of maximum penetration depth.

Results and Discussion

Solutions of Equation (1) were obtained using the Runge-Kutta method, and results for several values of particle size, velocity, and liquid surface tension are shown in Table 1 and Figures 2 & 3. Table 1 shows the maximum predicted extent of liquid surface indentation prior to either capture or rebound, and it is seen that such deformation is typically very shallow. Such a picture is at variance with the deep penetration capture models of

Pemberton and McDonald for non-wetted particles but in agreement with numerous published photographs of the particle/liquid interaction (e.g., Woffinden, et al., 1977). Trends in capture probability with surface tension and particle size are most clearly seen in Figure 2 & 3. Decreasing surface tension is seen to have a small negative effect on particle capture. As surface tension is lowered, the penetration depth increases, enlarging the area of the thinning film. The resulting increase in thinning time is greater than that in the interaction time, providing a possible explanation for an observed negative effect on collection efficiency of adding surfactant to the liquid.

The computations also predict that small particles are more readily collected than larger ones, but this result reflects the fact that the particles have been taken as smooth spheres. For most particulates, this assumption is not valid. Particles will usually be rough, and asperities on the particle surface will produce local thin spots in the vapor film leading to film collapse at much shorter times than predicted on the basis of a uniform film. The minimum size of asperities on a particle surface would probably be a more characteristic size parameter than the particle diameter.

Finally, increased impact velocity is also seen to decrease the capture probability. This is explained, as is the surface tension effect, by the increase in penetration depth leading to longer film thinning time.

Acknowledgement

This work was supported by funds from the Environmental Protection Agency administered as a subcontract of Meteorology Research, Inc., Altadena, California. The authors are indebted to Dr. L.E. Sparks of EPA and to Mr. G.J. Woffinden and Dr. D.S. Ensor of MRI for helpful discussions.

Nomenclature

- D = particle diameter, μm
- F = compression force on vapor film, dynes
- F_{μ} = viscous force resisting particle penetration, dynes
- F_{σ} = liquid surface force resisting particle penetration, dynes
- $\overline{F_{\sigma}}$ = F_{σ} averaged over the particle/droplet interaction time
- H = vapor film rupture thickness, cm
- M_p = particle mass, g
- $P(\theta)$ = dimensionless function of θ , defined in text
- R = particle radius, cm
- R = ratio of interaction time to film thinning time
- V = relative velocity between particle and collecting drop, cm/sec
- V_0 = "impact" velocity (V at time zero), cm/sec
- Z = particle penetration, cm (cf. Figure 1)
- θ = angular measure of particle penetration
- h = vapor film thickness, cm
- p = pressure, dynes/cm²
- r = radial coordinate
- t = time, sec
- z = axial coordinate
- θ = angular coordinate
- μ = liquid viscosity, poise
- σ = liquid surface tension, dynes/cm

Literature Cited

- Drees, W., Staub-Reinhalt. Luft, 26, 31 (1966).
- Ewers, W.E., Sutherland, K.L., Aust. J. Sci. Res., Series A, 5, 697 (1952).
- Fuchs, N.A., The Mechanics of Aerosols, pp. 338-352, MacMillan, New York, 1964.
- Goldshmid, Y., Calvert, S., A.I.Ch.E. J., 9, 352 (1963).
- Hesketh, H.E., J. Air Poll. Control Assoc., 24, 939 (1974).
- Lang, S.B., A Hydrodynamic Mechanism for the Coalescence of Liquid Drops, Univ. of California Lawrence Radiation Lab. Report No. UCRL-10097, Berkeley, 1962.
- Levich, V.G., Physiochemical Hydrodynamics, p. 395, Prentice-Hall, Englewood Cliffs, 1962.
- McDonald, J.E., J. Geophysical Res., 68, 4993 (1963).
- Pemberton, C.S., Int. J. Air Poll., 3, 168 (1960).
- Rabel, G., Neuhaus, H., Vettebrodt, K., Staub-Reinhalt. Luft, 25, 4 (1965).
- Taubman, A., Nikitina, S., Akad. Nauk SSSR, 110, 816 (1956).
- Taubman, A., Nikitina, S., Akad. Nauk SSSR, 116, 113 (1957).
- Weber, E., Staub-Reinhalt. Luft, 28, 37 (1968).
- Weber, E., Staub-Reinhalt. Luft, 29, 12 (1969).
- Woffinden, G., Ensor, D., Markowski, G., Sparks, L., "Interfacial Surface Effects on Particle Collection," Second Fine Particle Scrubber Symposium, New Orleans, May, 1977.

Captions to Figures

- Figure 1. Coordinate system for particle penetration.
- Figure 2. Ratio of interaction time to film thinning time, R , as a
function of liquid surface tension with particle diameter as
parameter (for an "impact" velocity of 7.6 cm/sec).
- Figure 2. Ratio of interaction time to film thinning time, R , as a
function of "impact" velocity with particle diameter as
parameter (for a liquid surface tension of 72.4 dynes/cm).

TABLE 1

<u>"Impact"</u> <u>Velocity</u> <u>(cm/sec)</u>	<u>Liquid</u> <u>Surface Tension</u> <u>(dynes/cm)</u>	<u>Penetration Depth/Particle Radius</u>
7.6	72.4	8.2×10^{-3}
"	60	9.0×10^{-3}
"	50	9.8×10^{-3}
"	40	1.1×10^{-2}
"	30	1.3×10^{-2}
"	20	1.6×10^{-2}
35	72.4	3.8×10^{-2}
64	"	6.9×10^{-2}

Dimensionless penetration depths (penetration depth/particle radius) for a 0.5 μm particle. (Impact velocities of 7.6 and 64 cm/sec are the terminal falling velocities in air of 50 and 200 μm water drops, respectively.)

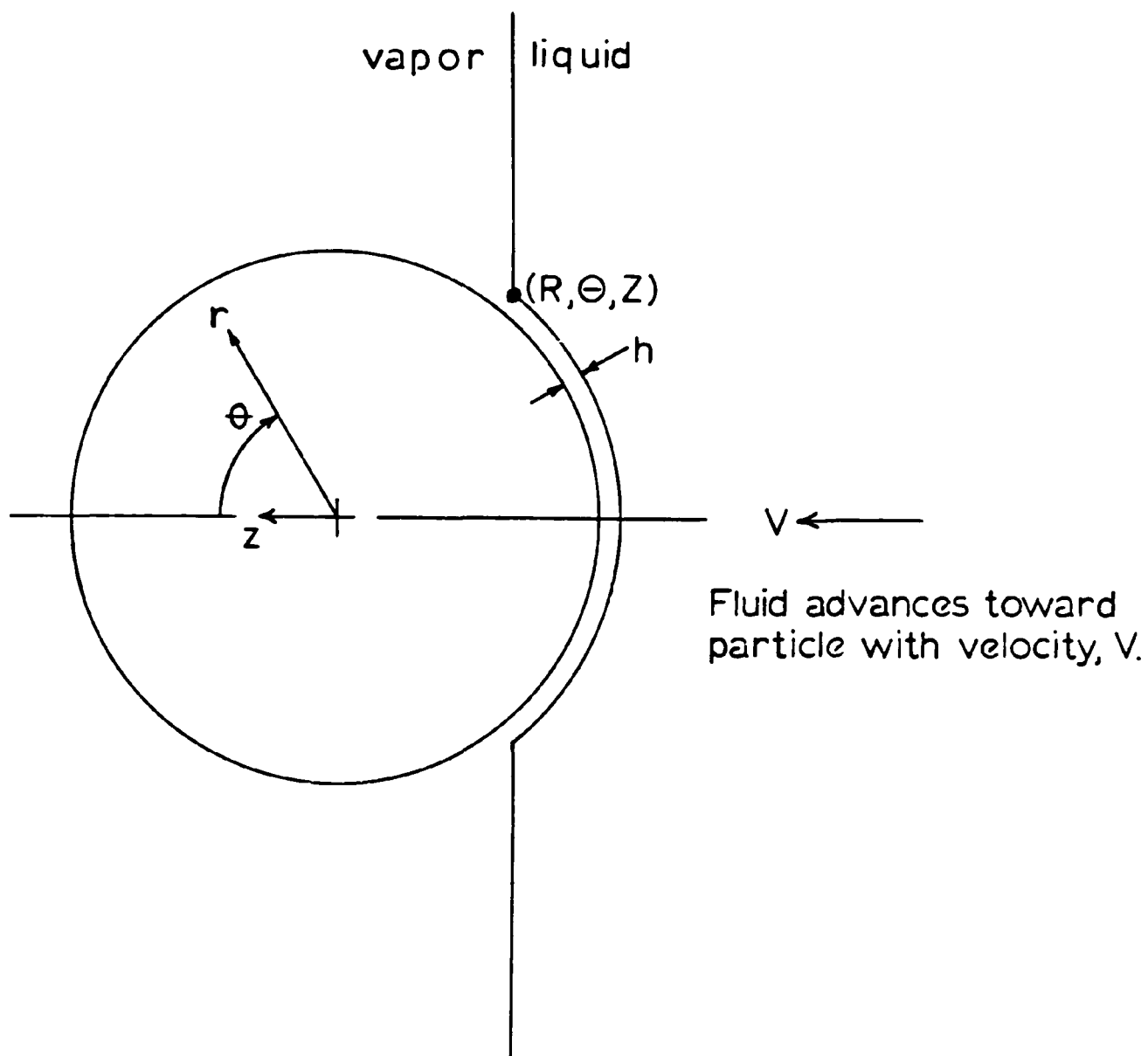


FIGURE 1

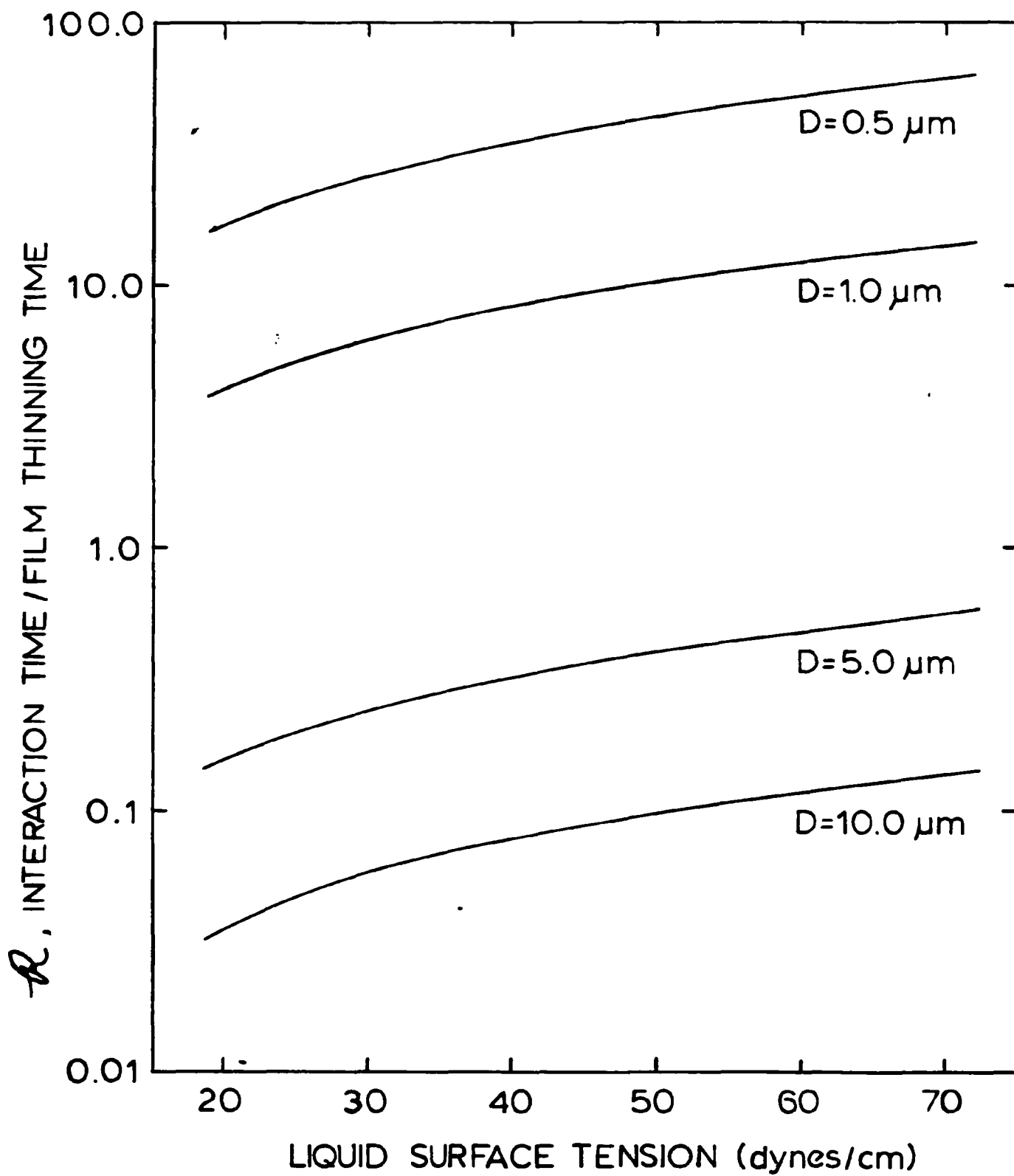


FIGURE 2

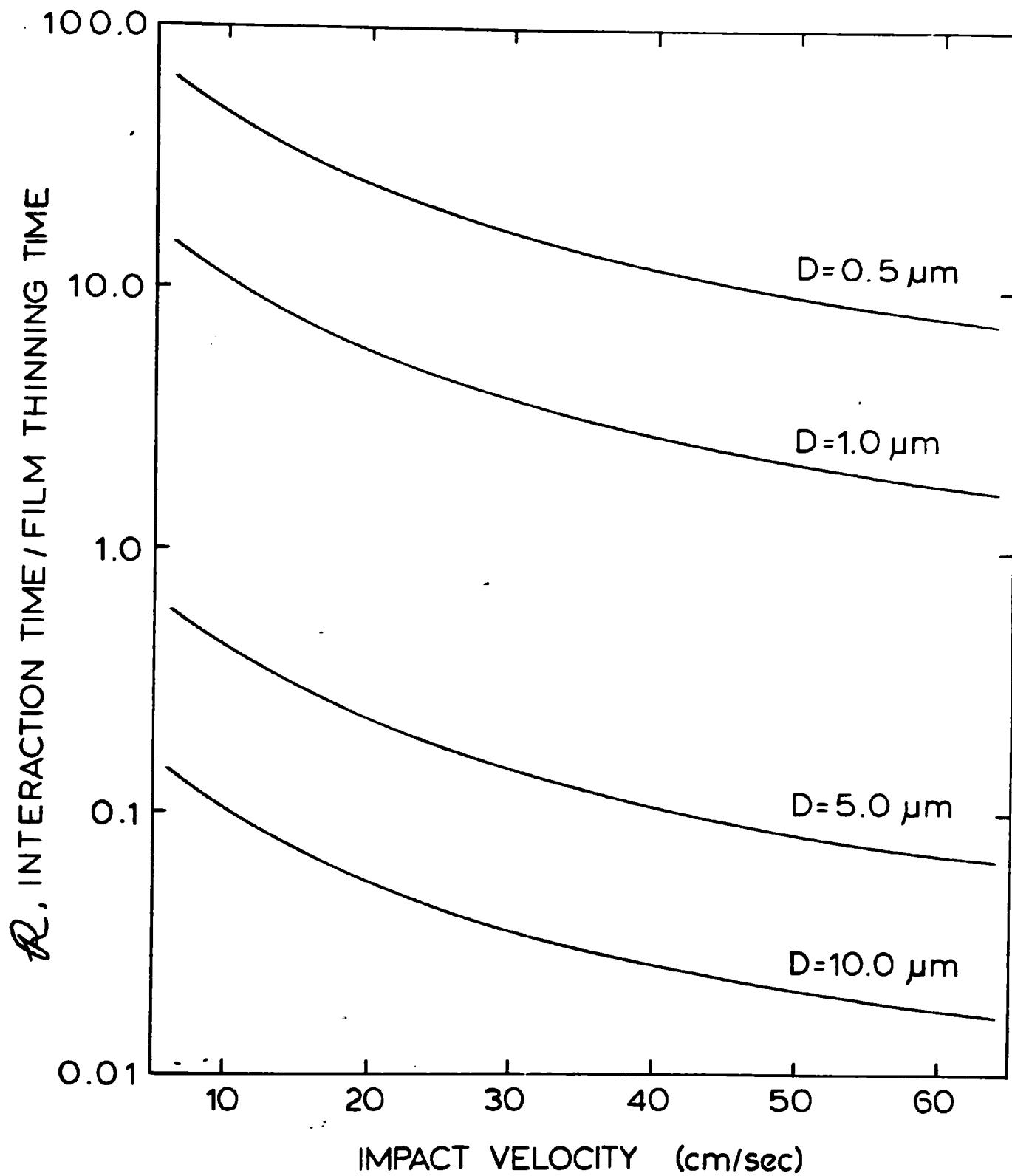


FIGURE 3

TECHNICAL REPORT DATA
(Please read instructions on the reverse before completing)

1. REPORT NO. EPA-600/7-78-097		2.		3. RECIPIENT'S ACCESSION NO.	
4. TITLE AND SUBTITLE Effects of Interfacial Properties on Collection of Fine Particles by Wet Scrubbers				5. REPORT DATE June 1978	
				6. PERFORMING ORGANIZATION CODE	
7. AUTHOR(S) G. J. Woffinden, G. R. Markowski, and D. S. Ensor				8. PERFORMING ORGANIZATION REPORT NO. MRI 77 FR-1503	
9. PERFORMING ORGANIZATION NAME AND ADDRESS Meteorology Research, Inc. P.O. Box 637 Altadena, California 91001				10. PROGRAM ELEMENT NO. EHE624A	
				11. CONTRACT GRANT NO. 68-02-2109	
12. SPONSORING AGENCY NAME AND ADDRESS EPA, Office of Research and Development Industrial Environmental Research Laboratory Research Triangle Park, NC 27711				13. TYPE OF REPORT AND PERIOD COVERED Final; 6/75-12/77	
				14. SPONSORING AGENCY CODE EPA/600/13	
15. SUPPLEMENTARY NOTES IERL-RTP project officer is D. L. Harmon, Mail Drop 61, 919/541-2925.					
16. ABSTRACT The report gives results of an analysis of typical wet scrubber models to determine the effects of surface tension on particle removal efficiency. Particle capture (removal) is a two-step process: collision of a particle with a spray droplet, and coalescence with the droplet. A change in surface tension of the scrubber water can influence both steps. The coalescence process (after a particle collides with a scrubber droplet) has been described by a film-thinning model that assumes that coalescence is controlled by the thinning rate of an air or vapor layer trapped between an impacting particle and droplet. If the film thins and ruptures before the particle rebounds, coalescence occurs. The thinning model predicts that a reduction in droplet surface tension allows deeper particle penetration into the droplet. The escaping vapor film therefore has a longer more resistive path, resulting in longer thinning times, thus reduced coalescence probability. When the surface tension of a scrubber liquid is modified, collection efficiency may be slightly improved or degraded depending on the spray droplet sizes and the sizes of particles being removed.					
17. KEY WORDS AND DOCUMENT ANALYSIS					
a. DESCRIPTORS		b. IDENTIFIERS/OPEN ENDED TERMS		c. COSATI Field/Group	
Air Pollution Dust Scrubbers Gas Scrubbing Mathematical Models Interfacial Tension		Efficiency Coalescing Air Pollution Control Stationary Sources Particulate Removal Efficiency		13B 14B 11G 07A, 13I 13H 12A 07D	
18. DISTRIBUTION STATEMENT Unlimited		19. SECURITY CLASS (This Report) Unclassified		21. NO. OF PAGES 71	
		20. SECURITY CLASS (This page) Unclassified		22. PRICE	